Full paper

Self-powered electronic skin based on the triboelectric generator

Haotian Chen[a], Yu Song[b], Xiaoliang Cheng[b], Haixia Zhang[a,b]

[a] *Academy for Advanced Interdisciplinary Studies, Peking University, Beijing 100871, China*
[b] *National Key Lab of Nano/Micro Fabrication Technology, Institute of Microelectronics, Peking University, Beijing 100871, China*

ARTICLE INFO

ABSTRACT

Human skin is the largest organ, which covers the human body and provides us the mechanical stimuli to help us interact with the outer environment. Inspired from the properties of human skin, imitating of the complicated human sensation using stretchable electronic devices becomes one of the most exciting research fields due to its vast potential application fields like wearable electronics, healthcare monitoring and artificial intelligence. To mimic real human skin, the huge sensor network is required to attach the body, where it seems critical to guarantee the energy supply at the same time. Nowadays, the emerging triboelectric nanogenerator (TENG), which can transduce the mechanical energy into the electrical energy based on the contact electrification and electrostatic induction, provides an attractive solution for the energy problem to work as the self-powered sensor. The self-powered sensor can generate electrical signal by itself, responsing to the stimulation from the environment without further energy supply devices. With four fundamental working modes and three main detection modes, TENG could develop versatile configurations to realize the various kinds of sensation. The mechanical compliance and stretchability together with the electrical conductance can be fulfilled beneficial from the advancement of material and micro/nano fabrication technology. In this way, the TENG based self-powered electronic skins (e-skins) have been developed with rational design to accomplish multifunctions of sensing including the pressure, position, strain, sliding and so on. It is expected that the self-powered e-skin will continue its fast development and make more progress to make the e-skin come into human life in the near future.

1. Introduction

Imitating of the complicated human sensation through electronic devices exerts the significant role to achieve the artificial intelligence (AI) and human machine interface (HMI) [1–3]. In the past decades, visual and auditory senses, have been successfully mimicked using the high-resolution camera and the high-fidelity microphone, which can be called the electronic eye (e-eye) and electronics hear (e-ear), respectively [4]. Additionally, human skin, which is responsible for the sense of touch, provides the most direct way for human to interact with the ambient environment safely and effectively.

The rapid development of new materials and micro/nano fabrication technology make the skin-like electronics possible by transducing the mechanical signal into electrical signal with the properties of flexibility and stretchability, which is usually called the electronic skin (e-skin) [5,6]. As it known to all, human body is fully covered by skin, with which every part of human body can sense the surroundings effectively. Similarly, e-skin is expected to be widely distributed in every aspect of human life and each part of human body, including the wearable electronics [7,8], personal health monitoring [9–11], artificial

prosthetics [12–14] and intelligent robots [15,16]. However, there still remains a lot of challenges, such as energy supply, stability, functionality and so on, to be solved to promote the e-skin from the laboratory research to industry. Among them, the most critical problem is the energy problem which is the essential part for all the modern electronics. Though battery is still the first choice for the electronic devices currently, the flexibility and stretchability limit its application, especially for e-skin working conditions. Moreover, the native drawbacks including the cyclically recharging, periodical maintenance and replacement and environmental pollution, become severer in the e-skin field.

One promising method to solve the above issue is the so-called self-powered sensing technology, which integrates the energy harvesting function and transducing function into one device [17–21]. On the one hand, such device can harvest energy from the living environment, especially from the human body, which is a huge energy source generated by physical motion and thermal emission. On the other hand, it can simultaneously respond to the change of the environment in the forms of electrical signals like voltage or current as an active sensor [22]. Many technologies associated with the self-powered sensing

E-mail address: hxzhang@pku.edu.cn (H. Zhang).

Table 1
Comparison of three mechanical energy harvesting techniques [27–31].

Type	Voltage	Current (μA)	Efficiency (%)	Advantages	Disadvantages
Electromagnetic	0.1–10 V	1–100 mA	5–90	High efficiency at high frequency, high current	Certain frequency, low performance at low frequency, heavy weight; material limitation (magnetic material), lack of flexibility, large size
Piezoelectric	1–200 V	0.01–10 μA	0.01–21	High sensitivity, easy to be integrated into micro fabrication, flexible	Low efficiency; material limitation (piezoelectric material), lack of stretchability,
Triboelectric	1–1500 V	10–2000 μA	10–85	High efficiency, high output voltage, no material limitation, low-cost, flexible and stretchable	Sensitive to external environment; friction damage

including photovoltaic effect [23], thermoelectric effect [24], electromagnetic effect [25], piezoelectric effect [26] and triboelectric effect [27], have been deeply explored to convert the surrounding energy into electrical energy effectively. Among them, electromagnetic effect, piezoelectric effect and triboelectric effect, which all can transform the mechanical energy into the electrical energy, are regarded as the candidates for designing the self-powered e-skin, of which the main function is to reflect the change of different kinds of force. Table 1 summarizes the three mechanical energy harvesting techniques [28–32]. From the comparison, triboelectric based self-powered sensor is regarded as the most promising method in wearable electronics due to its simple and diversified structure compared to the electromagnetic device and its almost limitless choice of materials and higher performance compared the piezoelectric device [33–35]. First proposed in 2012, triboelectric nanogenerator (TENG) [27] has been dramatically developed in the following years and exhibits its attractive potential in the energy harvesting and self-powered sensing due to its outstanding characterization including high-output performance low cost, excellent versatility in structural design and sustainability [36–38].

In this review, we primarily focus on the current strategies and technologies for achieving the triboelectric based self-powered electronic skin with a variety of functions (Fig. 1). First, we introduce the working mechanism of the triboelectric based self-powered sensor to demonstrate the basic working modes and detection modes. Furthermore, the design principle of the e-skin, which must meet the requirements of electrical conductance and mechanical compliance simultaneously, is also covered. In the end, we summarize the various applications and recent trends and look forward to the next-generation development.
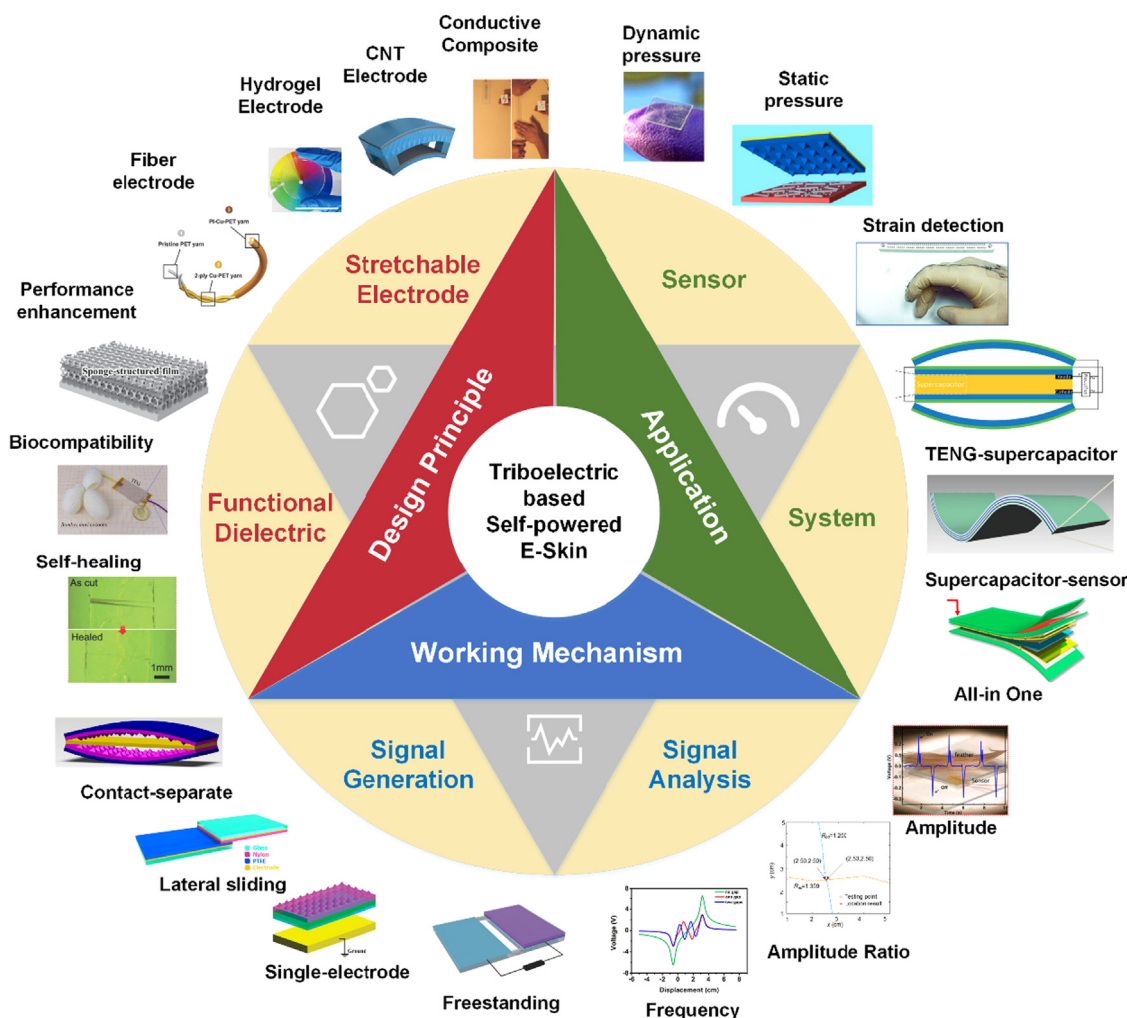
2. Working mechanism

For any electronic device, the signal generation and analysis are two basic issues when designing the self-powered sensor. In this section, we will first discuss the working mechanisms of TENG to understand the characterizes of different working modes. Then, according to the signal generated by TENG, we will introduce the main sensor types utilized in TENG and their detection methods. With different configurations of the working mode and detection mode with proper structure design, multiple functions can be achieved using the triboelectric based self-powered sensor.

2.1. Signal generation

TENG works based on the coupling effect of contact electrification and the electrostatic induction. The contact electrification describes a phenomenon that two different materials get surface charges with opposite polarity, which is called the triboelectric pair, after they contact with each other. By placing two electrodes on the backside surface of the triboelectric pair, the charges will move between these two electrodes due to the electrification induction effect when the triboelectric pair moves. In this way, with the help of TENG, the external motions can generate an electrical signal by converting the mechanical energy into the electrical energy without other energy supply. Four fundamental working modes of TENG have been established according to different operating principle including the contact-separation (CS) mode [39,40], lateral sliding (LS) mode [41,42], single-electrode (SE) mode [43,44] and freestanding (FS) mode [45] (Fig. 2**(a)**).

2.1.1. Contact-separation mode

The CS mode is the first fundamental mode of TENG [46], which consists of two kinds of materials with different triboelectric polarities and two electrodes placed on their backsides. Under the external pressure, two materials contact with each other to generate surface charges due to the contact electrification effect. According to the triboelectric series, which shows the tendency to lose electrons or gain

Fig. 1. Overview of this review including the working mechanism, design principle and application. "Contact-separate". Reproduced with permission from American Chemical Society (2013) [39]. "Lateral sliding". Reproduced with permission from American Chemical Society (2013) [42]. "Single-electrode". Reproduced with permission from Royal Society of Chemistry (2013) [44]. "Freestanding". Reproduced with permission from Wiley (2014) [45]. "Frequency". Reproduced with permission from Elsevier (2017) [60]. "Amplitude Ratio". Reproduced with permission from American Chemical Society (2016) [58]. "Amplitude". Reproduced with permission from American Chemical Society (2012) [47]. Copyright 2012, American Chemical Society. "All-in-one". Reproduced with permission from American Chemical Society (2016) [130]. "Supercapacitor-sensor". Reproduced with permission from Wiley (2017) [129]. "TENG-supercapacitor". Reproduced with permission from Royal Society of Chemistry (2016) [128]. "Strain detection". Reproduced with permission from Wiley (2015) [112]. "Static pressure". Reproduced with permission from American Chemical Society (2013) [115]. "Dynamic pressure". Reproduced with permission from American Chemical Society (2014) [56]. "Conductive composite". Reproduced with permission from Wiley (2016) [81]. "CNT electrode". Reproduced with permission from Wiley (2014) [75]. "Hydrogel electrode". Reproduced with permission from American Association for the Advancement of Science (2017) [87]. "Fiber electrode". Reproduced with permission from Wiley (2016) [94]. "Performance enhancement". Reproduced with permission from Wiley (2012) [99]. "Biocompatible". Reproduced with permission from Elsevier (2016) [104]. "Self-healing". Reproduced with permission from Wiley (2018) [108].
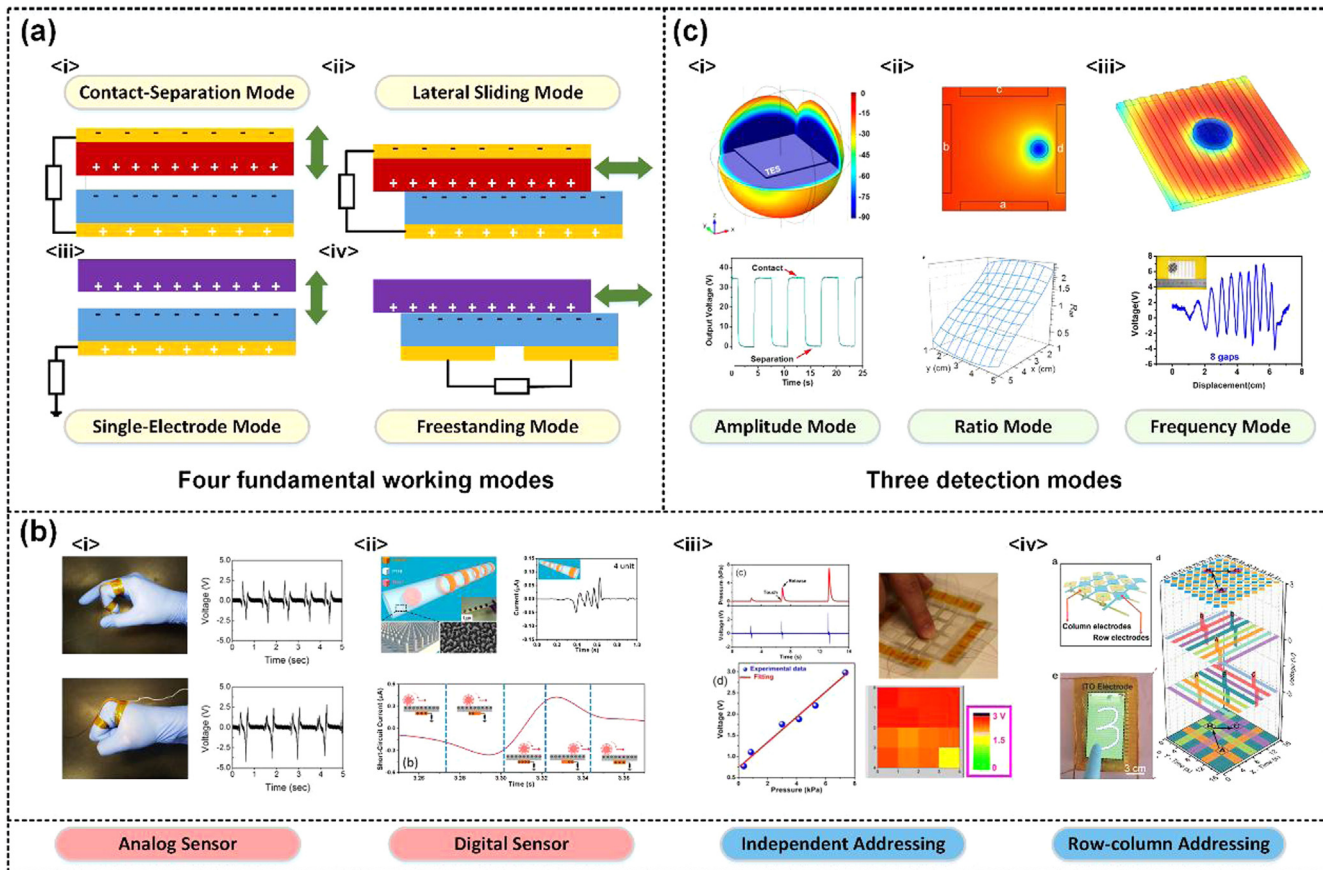
electrons of various common materials, one material of the triboelectric pair shows positive potential while the other shows negative potential with the same amount. When the external pressure is releasing, the triboelectric pair separate and an internal potential is established, which drives the charges flowing from one electrode to the other through the connected load to keep the balance of the electrical potential due to the electrostatic induction. Thus a transient current is generated. When the external pressure applied again to close the gap, the induced charges flow back to their original electrode, which also generates a transient current with opposite direction. CS mode TENG can generate a periodical alternative electrical output when repeating the CS process. CS mode TENG is the most convenient way to demonstrate its pressure sensing capability. The first self-powered pressure sensor [47] is achieved with the CS mode TENG, which can detect gentle pressure as small as a feather (0.4 Pa) through the contact of two polymer sheet.

2.1.2. Lateral sliding mode

The LS mode TENG [42] has the similar structure with CS mode. The electricity is also generated through the contact and separation between the triboelectric pair. The only difference is that the CS mode requires the two materials to separate in the vertical direction while the LS mode requires the two materials to separate in the in-plane direction. Compared to the CS mode, the most attractive advantage of LS mode is that it could operate under very high frequency with proper structure design, which is beneficial for enhancing the efficiency.

2.1.3. Single-electrode mode

The two modes introduced above have two electrodes attached onto the moving triboelectric layers, which brings inconvenience in some application fields. The SE mode TENG is introduced to solve this problem [44]. Different from the other TENG, SE mode TENG has only one electrode and one triboelectric layer. It employs an external object such

Fig. 2. The summary of the basic working modes of TENG, signal types of TENG and detection modes of the self-powered sensor. (a) Based on the operation mechanism, TENG can be classified into four fundamental working modes including contact-separate mode, lateral sliding modes, single-electrode mode and freestanding mode. (b) Analog and digital types for individual device and independent and row-column addressing methods for array device. Reproduced with permission from Elsevier (2017) [52], American Chemical Society (2014) [53], American Chemical Society (2013) [54] and Wiley (2016) [55], respectively (c) According to the requirement for designing the specific functioned self-powered sensor, there are three detection modes: amplitude mode, ratio mode and frequency mode. Reproduced with permission from American Chemical Society (2014) [56], American Chemical Society (2016) [58] and Elsevier (2017) [69], respectively.

as human skin as the other triboelectric layer to interact with itself. The electrode is connected to the ground through the load and the current will flow between the electrode and the ground when the external object moves. In this way, the SE mode TENG can detect the movement of the outer object while it remains static. Though the SE TENG has the simplest structure and is very easy to integrate with other electronics, the conversion efficiency can only reach 50% [48]. What's more, as any object such as human finger [49], can work as the triboelectric layer, the SE TENG is usually designed as a touch sensor to avoid the different amplitudes caused by different contact objects.

2.1.4. Freestanding mode

FS mode is the last mode of TENG, in which the two electrodes are fixed while an external object can move freely between these two electrodes [45]. According to the theory, the energy conversion efficiency of FS mode TENG can reach 100% [50]. As the moving object can separate from the electrode part, FS mode is suitable for detecting the motion of a moving object. In addition, by designing proper structures like grating structure [51], the electrons can transfer between the electrodes several times, thus generating an alternative current (AC) with higher frequency, which can provide more information for further analyzing.

2.2. Signal type

According to the working modes mentioned above, the signal type is the next consideration for designing a functional sensor. For an

individual sensor, the signal generated can be classified into analog sensor and digital sensor based on the target we need to detect. Furthermore, multi individual sensors could construct a sensor array to reflect the situation across a large area. As the result, two addressing modes, independent addressing mode (IA) and row-column addressing mode (RCA), are also reviewed.

2.2.1. Individual sensor

2.2.1.1. Analog. TENG based analog sensor is the most frequently used sensor especially for detecting mechanical related signals such as pressure and strain. The analog sensor usually directly adopts the peak-peak value to reflect the physical signal. In addition, the waveform of the output analog can also be analyzed to tell the different kinds of motions. Kim and his co-workers used gold-nanosheet as electrode and patterned pyramidal PDMS as dielectric to fabricate a human motion sensor [52]. This device shows excellent electrical output stability against a large number of repeated push/leasing cycles. The maximum output voltage ranges from 39.4 to 98.9 V with the increasing of pushing force from 1 to 6 N due to the changed contact area of the microstructured PDMS. What's more, by analyzing the waveform of the output voltage, this self-powered sensor can tell the difference between several human motions including index finger, knuckle and wrist (Fig. 2(b) < i >).

2.2.1.2. Digital. Digital self-powered is usually adopted for measuring the movement related information by simply detecting the number of the output cycles. Su et al. reported a self-powered displacement sensor

to detect the movement of a charged ball in a tube as shown in Fig. 2(b) < ii > [53]. The tube is wrapped with ring shaped copper electrodes. As the charged ball flow close to the electrode, the electrons will transferred between the copper and the ground to generate the alternating output. When the distance between the neighboring electrodes is fixed, the displacement of the charged ball in the tube can be easily calculated by multiplying the number of cycles with the distance, which provides an efficient and stable method for tracking the movement of a charged object.

2.2.2. Sensor array

Sensor array is a group of sensors with standard geometry pattern. By extending from a single device to multi sensors, the array adds new dimensions for collecting and detecting more parameters and provides more information. Independent addressing and row-column are two main addressing methods

2.2.2.1. Independent addressing.
Independent addressing is the simplest addressing method. Every sensor in the array has an independent transmission line. The advantage is each of the sensor can retain its own characterizes with easy wiring pattern. Yang et al. proposed a matrix of independently addressable TENGs, each of which is composed two ITO electrodes and one microstructured PDMS working as the dielectric between the electrodes shown in Fig. 2(b) < iii > [54]. In this way, the tactile information including the position and the pressure can be determined by analyzing the output voltages of each pixel. The detection sensitivity of the pressure is around 0.29 V/kPa. As each sensor works independently, this sensor array supports the multi-point touch detection and each pixel can detect the pressure precisely. However, for a sensor array consisting of $m \times n$ sensors, where m is the number of sensor in a row and n is the number of sensor in a column, the number of addressing would be rather complex when m and n are large

2.2.2.2. Row-column addressing.
Row-column addressing is the method widely applied in the traditional electronic device array such as memory. This method can significantly reduce the number of addressing lines from $m \times n$ to m + n, which greatly shortens the measurement period and simplifies the wiring complexity. Wang et al. reported a self-powered, high-resolution pressure sensor array with RCA method (Fig. 2(b) < iv >) [55]. Voltage signals can be measured from both the corresponding row and column lines when an object contacts the intersection. The drawback of RCA method is also obvious. The array can't distinguish multi-point and single-point and the pressure can not be exactly reflected by the voltage if the contact point is not on the intersection. As the result, different addressing methods should be carefully chosen for achieving different functions.

2.3. Detection mode

When considering the self-powered sensing of TENG based device, three kinds of detection modes, amplitude mode (AM) [56,57], ratio mode (RM) [58,59] and frequency mode (FM) [60,61], are developed (Fig. 2(b)).

2.3.1. Amplitude mode
Among the three detection modes, AM is the most common one because this mode is most similar to the TENG based energy harvester. The first self-powered TENG sensor works based on this detection mode, which used the output amplitude of the TENG to reflect the pressure [47]. Following this work, many groups have designed a lot of AM self-powered sensor to detect various signals like vibration [62–64], rotation [65,66], acceleration [67] and so on.

Amplitude can provide plenty of information for detecting various signals, however, TENG is susceptible to lots of environment elements like temperature, humidity [68]. Furthermore, the materials contacted

with the device can also influence the final results of the amplitude from TENG due to contact electrification effect. For example, polytetrafluoroethylene (PTFE) contacted with the PI with gentle pressure and rubber contacted with the PI with large pressure may generate similar amplitude. Such phenomenon is acceptable in energy harvester but may cause inaccuracy for sensing.

2.3.2. Ratio mode
As AM is usually disturbed by external elements, RM was proposed to solve this problem. RM needs two or more TENGs in the sensing system to compare the amplitudes in ratio. The variation caused by the environment or the material can be eliminated by the ratio. For instance, Zhang et al. proposed an analogue smart skin to detect the touch position in a plane with four pieces of conductors working as electrodes for four SE mode TENGs [58]. This touch sensor uses the amplitude ratio of the opposite TENGs to detect the position in one dimension (1D). With two pairs of opposite TENGs, a two-dimension (2D) touch sensor can be achieved by the two ratio to reflect the coordinates in the plane.

2.3.3. Frequency mode
Though it will not be influenced by the external elements, RM loses a lot of information in the waveform, especially, the time information. Different from RM, FM, which ignores most of the amplitude information, is dependent on the waveform and frequency as a digital sensor. FM can retain the time information, which contains lots of important information like contact process and release process. Although the FM still need the waveform, the concrete number of the wave amplitude, which may be easily impacted by the outer elements, will not be taken into the analysis. Based on this detection mode, the TENG based sensor can reflect some dynamic physical characteristics like sliding motion [60,61] or roughness detection [69].

When designing self-powered sensors with specific functions, different working modes and detection modes should be taken into account at the same time to maximum their characterizes and advantages to obtain the optimal results.

3. Design principle

Human skin can be considered as the benchmark when designing the e-skin [70,71]. The basic consideration for developing e-skin is the choice of materials, which are able to mimic the natural properties of human skin such as flexibility and stretchability. In additional to the mechanical compliance, e-skin requires that the signal can be transmitted to the external instrument for further analyzing. Thus, the electrical conductance is equally important when design the e-skin.
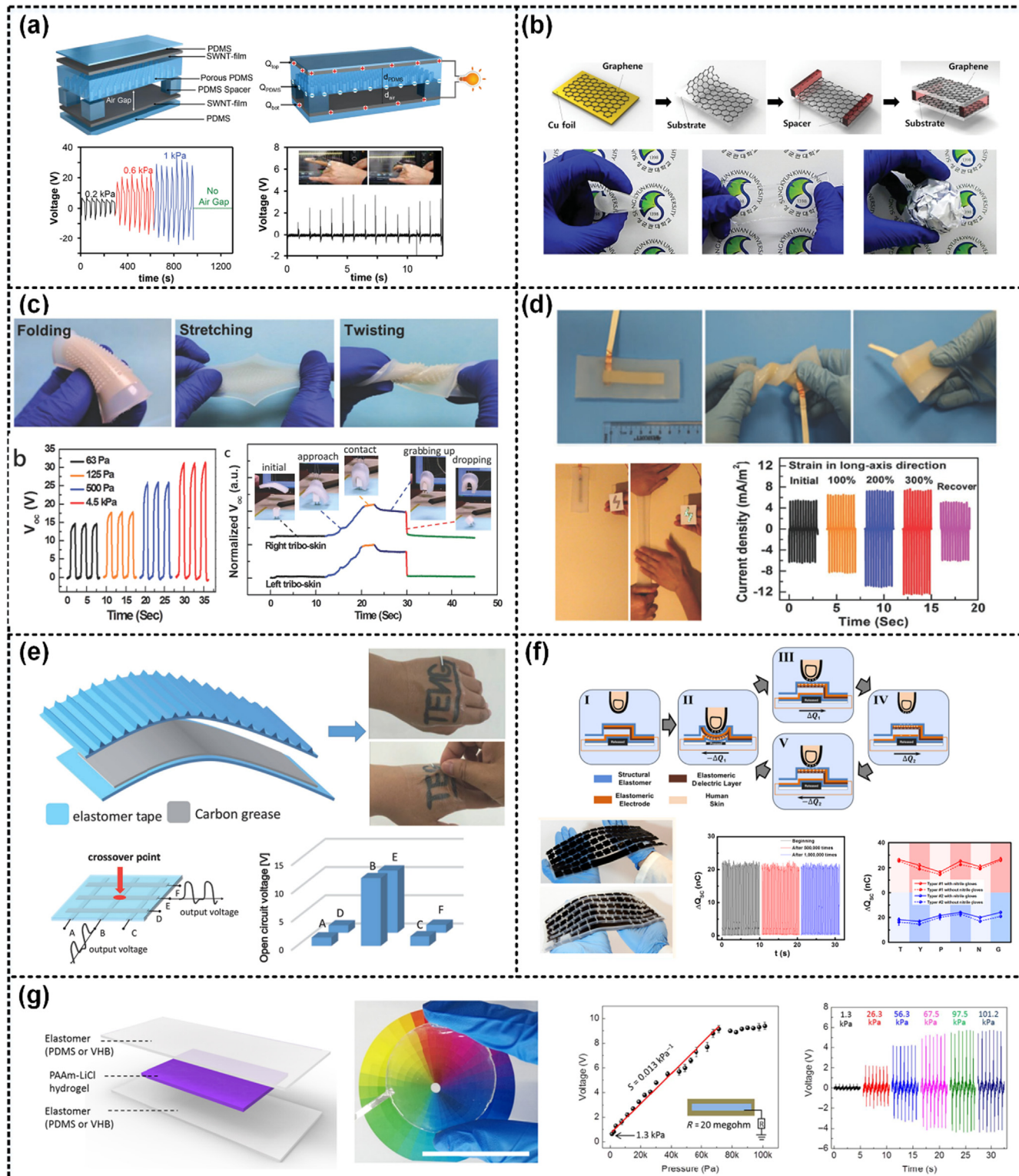
For every TENG, electrode and dielectric are two indispensable parts composing the whole device. When designing the TENG based e-skin, the properties of electrode and dielectric should be considered separately due to their different requirements. As the result, in the following section we discuss the design principle of electrode and dielectric, respectively.

3.1. Design of electrode

For the electrode, the most significant problem is how to develop the flexible and stretchable conductive materials as traditional electronics usually adopts metal as electrodes, which could not fulfill the requirement of e-skin. Developing new materials and constructing new structure are two main routines for achieving this target [72].

3.1.1. Material
Material is the fundamental block for constructing all the devices. Development of new material and corresponding processing method are very critical for achieving the stretchable conductor. In addition to the mechanical compliance and electrical conductivity, the compatibility

Fig. 3. Design of stretchable electrode with new materials. (a) A stretchable energy harvesting e-skin which can detect, differentiate and harvest a variety of mechanical stimuli with CNT film as the electrode layer. Reproduced with the permission from Wiley (2014) [75]. (b) A graphene based transparent, flexible TENG with different numbers of layers. Reproduced with permission from Wiley (2014) [76]. (c) A self-powered, highly stretchable and sensitive triboelectric e-skin with Ag flake-Eco-flex conductive composite as stretchable electrode. Reproduced with permission from Wiley (2018) [80]. (d) An electric eel-skin inspired super-stretchable e-skin with the AgNW-silicon rubber working as the ultra-stretchable conductor, which can sustain 300% strain. Reproduced with permission from Wiley (2016) [81]. (e) A carbon black grease based TENG which can cover on human skin tightly. Reproduced with permission from Wiley (2017) [82]. (f) A CNT-PDMS based TENG with a keyboard cover shape to harvesting and distinguish the daily typing activity. Reproduced with permission from American Chemical Society (2016) [83]. (g) An ultra-stretchable transparent TENG based self-powered e-skin using ionic conductive PAAm-LiCl hydrogel as the electrode. Reproduced with permission from American Association for the Advancement of Science (2017) [87].

with large-area processing and cost should also be taken into consideration. Nanomaterials with plenty of attractive properties have provided us a very good option. What's more, emerging materials like hydrogel also have attracted a lot of attention due to their unique performance. Below, we survey several of the most commonly used materials for fabricating the stretchable electrodes of TENGs.

3.1.1.1. Carbon based nanomaterial. Carbon based material is the great candidate for the electrode because of their low-cost, abundancy and comparatively good conductivity. In recent years, the discovery of new carbon allotrope including carbon nanotube (CNT) [73] and graphene [74] has attracted much attention in the materials research field due to their unique electronic and mechanical properties. CNT has remarkably high length-radius ratio, which can form the stretchable conductive film with low percolation threshold. In 2014, Bao et al. developed the CNT-based TENG which can generate voltage and current in the range of tens of volts and tenths to several $\mu A\ cm^{-1}$, respectively, as shown in Fig. 3(a) [75]. What's more, it can also work as a self-powered pressure sensor, with a high pressure sensitivity of 1.5 kPa^{-1} under 1kPa with the largest stain of 30%. Graphene based flexible TENG, demonstrated by Kim and his coworkers, also shows great flexibility and stretchability due to its atom-level thickness as shown in Fig. 3(b) [76]. Several kinds of TENGs are fabricated based on one-layer, two-layer, three-layer and four-layer graphene. Among them, one-layer graphene based TENG shows the highest output voltage and current density of 5 V and 500 nA, respectively, which can be explained in terms of their work function and friction.

3.1.1.2. Conductive composite. Conductive composite is developed by introducing conductive fillers into elastomer, which combines the electrical property and mechanical stretchability into a whole material. The most important issue for the conductive composites is how to disperse the conductive fillers uniformly into the elastomer [72].

Metal is the most common electrode materials in the electronics owing to their exceptionally high conductivities. However, bulk metals are rigid and easy to break under strain. Nano-scale metal materials such as nanoflake [52,77] and nanowire [78,79] are developed, showing excellent performance in the stretchable conductors. Among all kinds of metals, Ag is the most attractive material in the stretchable electronics due to its high conductivity. Lai et al. demonstrated a pressure sensor based on the TENG with the silver flake (Ag flake) network working as the stretchable electrodes as demonstrated in Fig. 3(c) [80]. Penetrated into the Eco-flex silicone rubber, the Ag flake based self-powered sensor can maintain its sensing ability under 100% strain with the excellent sensitivity of 0.29 kPa^{-1} in low-pressure regime (< 5 kPa) and lowest detection limit to 63 Pa. Besides the Ag flake, silver nanowire (AgNW) is another commonly used material. Compared with Ag flake, the stretchability of AgNW film is better because its highly anisotropic in size allow good electrical performance at lower filler concentration according to the percolation theory. In 2016, a skin-like durable TENG was developed with the AgNW electrode, which was embedded in the silicon rubber, showing a lot of attractive properties including biaxial including biaxial stretchability, uniaxial stretchability of over 300% strain as well as the capabilities to multiple twists and folds and various desired deformations (Fig. 3(d)) [81].

Besides the metal nanomaterial, carbon based material is also a kind of successful conductive filler for stretchable conductor. Carbon black is one of the least expensive available conductive filler. Chen et al. have developed a SE TENG composed of two commercial VHB elastomer and a carbon grease layer sealed in the two VHB films demonstrated in Fig. 3(e) [82]. This device can be attached on a human hand tightly. As its thickness is only 102 μm, this device can work durably under a strain of 100%. However, as the conductivity of carbon black is very low ($\approx 0.5\ S\ cm^{-1}$), which limits its application fields, CNTs based conductive composites emerge in recent years and show excellent electrical

performance in stretchable electronics. In 2016, a fully elastomeric TENG in form of keyboard cover was proposed by Li et al. shown in Fig. 3(f) [83]. Sealed between two elastomer dielectric, a conductive elastomeric film was fabricated by mixing the platinum-catalyzed silicone Ecoflex 0500 with carbon and CNT to ensure good flexibility and stretchability. The sheet resistance of this conductive composite is about 843 Ω without any strain.

3.1.1.3. Hydrogel. Composed of hydrophilic polymer networks swollen with water or ionic aqueous solution, hydrogels are the kind of materials in solid form, soft, stretchable and biocompatible. Suo and his coworker have made great contribution in this field [84–86]. Many stretchable functional devices have been demonstrated with ionic hydrogels as the electrode conductor like strain sensor and loudspeakers [86]. Similarly, hydrogel can work as the TENG electrode as well. Pu et al. reported a skin-like TENG with elastomer and ionic hydrogel working as the electrification layer and electrode respectively (Fig. 3(g)) [87]. This device can not only harvest biomechanical energy but also sense touch. The electrode is polyacrylamide (PAAm) hydrogel containing lithium chloride (LiCl) and two commonly used elastomers, polydimethylsiloxane (PDMS) and 3 M VHB 9469, are adopted as the dielectric material. This device show ultrahigh strechability (strain of 1160%) and highly transparency (96.2%). Additionally, working as a sensor, this device can detect pressure as low as 1.3 kPa.
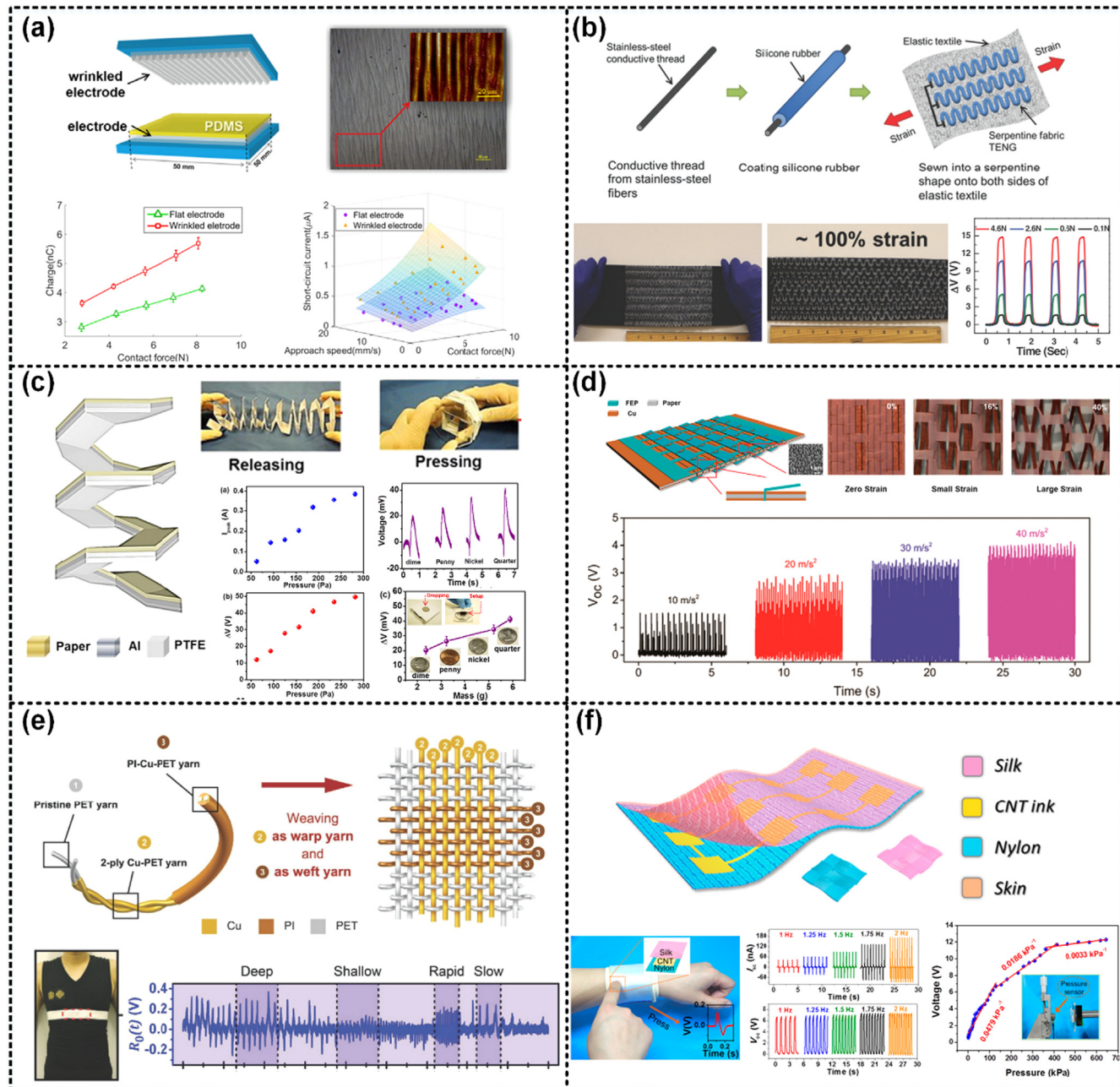
3.1.2. Structure

Besides the new material, structure design is another important method to obtain the stretchable conductor. Proper structure design enables rigid materials to extend along the stretching direction without failure. We will introduce three major approaches to constructing the stretchable structures: 2-dimension (2D) geometric design, 3-dimension (3D) geometric design and fiber/textile design.

3.1.2.1. 2D geometric structure. 2D geometric design mainly concentrates on the special structure on the surface of a material. Wrinkle is one of the most common and simple structure for constructing stretchable devices. Depositing a high-modulus thin film onto a pre-strained soft substrate can produce the wrinkle structure after the strain is released from the substrate. This wrinkle structure can ensure the high-modulus film to be stretched to the pre-strained state [88]. The wrinkle structure can also obtained by shaping the wave structure on the elastomer substrate before the film deposition, which do not need the pre-strain process [89]. Choi et al. proposed a roll printing process for fabricating the wrinkled Ag electrode used for TENG [90]. This method not only endow the Ag electrode with the stretchability, but also increase the quantity of triboelectric charges and outpour power with 37% and 120% due to larger contact areas compared with the flat electrode (Fig. 4).

Another common 2D structure for constructing stretchable electronics is serpentine. The strain reduction in this structure is dependent on the patterned geometry and material properties. Lai et al. reported a stretchable TENG based self-powered sensor by sewing the stainless-steel thread electrode into a serpentine shape on an elastic textile as shown in Fig. 4(b) [91]. Due to the special design of the structure, this sensor can endure a strain up to 100%. By shaping into a glove, this device can identify the digital gesture.

3.1.2.2. 3D geometric structure. Different from the 2D geometric design, 3D geometric design is associated with the whole material. Though 3D design brings about more complex fabrication process, the performance is better than 2D as a compensation. In particular, the 3D structures in TENG based devices usually have some distinctive functions. When the device is stretched, the deformation of 3D structure usually results in the obvious change of distance between two neighboring charged parts, which can work as a TENG based sensor to detect this movement. Yang

Fig. 4. Design of stretchable electrode with new structures. (a) A roll-printed wrinkle electrode for adoption in a TENG. Reproduced with permission from IOP Publishing (2015) [90]. (b) A single-thread based wearable TENG sensor with serpentine shaped highly stretchable electrode. Reproduced with permission from Wiley (2016) [91]. (c) An Origami shaped highly stretchable TENG. Reproduced with permission from American Chemical Society (2015) [92]. (d) A Kirigami shaped highly stretchable TENG. Reproduced with permission from American Chemical Society (2016) [93]. (e) A washable, stretchable TENG for human respiratory monitoring through loom weaving of metallic yarns. Reproduced with permission from Wiley (2016) [94]. (f) A textile based self-powered triboelectric gesture monitoring self-powered sensor utilizing conductive CNT ink and screen-printing technology. Reproduced with permission from American Chemical Society (2018) [96].

et al. developed a paper based slinky TENG with origami configuration for pressure detection as shown in Fig. 4(c) [92]. Composed of three layer, paper substrate, PTFE thin film, and aluminum foil, the device seems like a spring, so it owns good stretchability. With external force applied and released, the neighboring paper and PTFE contact and separate periodically, thus generating voltage signal, which can reflect the quantity of the pressure. Another 3D structure paper based TENG is proposed by Wu et al. with the kirigami pattern (Fig. 4(d)) [93]. Compared with the origami pattern, this pattern is more robust to response to the external pressure. This device, which is made from nonstretchable material, can sustained an ultrahigh tensile strain up to 100%.

3.1.2.3. Fiber/textile structure. No matter whether the natural materials such as silk and cotton or man-made fiber materials like nylon, they all exhibit excellent mechanical compliance, which people can wear comfortably. Inspired from the patterns of textile, researchers have done lots of works to construct the conductor into this structure to make them stretchable. Conductive textile can be fabricated by weaving plenty of fibers together. Hu et al. reported a textile TENG based self-powered sensor for detecting human respiratory information including rate and depth as shown in Fig. 4(e) [94]. This device was fabricated by

direct weaving of Copper (Cu)-coated polyethylene terephthalate (Cu-PET) warp yarns and polyimide (PI)-coated Cu-PET (PI-Cu-PET) weft yarns on an industrial sample weaving loom. Besides its great sensing ability, it also shows a remarkable washing durability, which can withstand standard machine washing tests.

Another common method for obtaining conductive textile is directly coating conductive materials on the traditional textile, which provides a simple and low-cost fabrication process [95]. Cao et al. proposed a screen-printed washable electronic textile as the self-powered touch triboelectric sensor, as shown in Fig. 4(f) [96]. This device is composed of three layers. The top layer and bottom layer are silk fabric and nylon, respectively. Between two dielectric layers, a CNT-nylon layer works as the electrode with conductivity of $0.2\,k\Omega/\square$. Owning to the rough surface of textile, this device shows high sensitivity and fast response to external force. Incorporated into a glove, this device can detect different gestures serving as a smart home controller.

3.2. Design of dielectric

Different from the electrode, the strechability of dielectric is not the main issue as many conventional elastomers like PDMS can work as the stretchable dielectric. The main purpose of designing dielectrics is to develop the high signal-noise ratio (SNR) e-skin by enhancing the output of TENG. In addition, some other properties like biocompatibility humidity-resistant and self-healing, are also very important issues for development of the self-powered sensors.

3.2.1. Performance improvement

For TENG self-powered sensors, the noise is crucial for performance and accuracy. As the TENG is sensitive to many elements, the sensing signals are usually interfered by them and the final result is not accurate. As the result, improvement of the output of the TENG based self-sensor is the primary target to enhance the SNR. Based on the working mechanism of TENG, contact area and surface charge density are two main parameters to influence the output. Many groups have contributed a lot of works to improve the output based on the two aspects.

3.2.1.1. Microstructure.
Introducing microstructures into the design of dielectric in TENG is a promising option to increase the contact area [97,98]. The first TENG based self-powered sensor reported by Wang et al. have compared various PDMS pattern arrays to enhance the friction effect as shown in Fig. 5(a) [47]. In particular, the PDMS films with pyramid or cube structures give almost 5–6 times improvement in output compared with that in the unstructured films, which demonstrates that the microstructure on the surface can effectively improve the output. Besides the microstructure on the surface, 3D microstructure can also effectively increase the performance. A sponge structured TENG was proposed in 2014 by Baik and Kim [99]. The sponge structure is achieved by removing the compactly arranged polystyrene (PS) nanoparticles from the PDMS film, as shown in Fig. 5(b). From the experiment, the output voltage and current density of sponge structure TENG can reach 130 V and $0.10\,mA\,cm^{-2}$, respectively. Comparatively, TENG without the sponge structure can only ontain 50 V output voltage and $0.02\,mAcm^{-2}$ current density. What's more, by comparing different sizes of PS nanoparticles, the electrical output performance of the TENG increases with the decrease in the pore size diameter, due to the rapidly increased contact area.

3.2.1.2. Material.
The triboelectric series shows that different materials have different tendency for losing electrons or attracting electrons, which give us the reference for choosing proper materials to improve the performance [37]. Zhang et al. proposed a fluorocarbon plasma treated PDMS working as the dielectric of TENG shown in Fig. 5(c) [100]. The element Fluorine, which has the strongest electronegativity, is usually chosen as one of the triboelectric pair to attract electrons. However, fluoropolymer seldom has very good mechanical compliance,

which is necessary in electronic skin. In order to solve this problem, the research group adopted a single-step fluorocarbon plasma to treat the uncured PDMS. This method, not only successfully coated the fluoropolymer on the soft PDMS, which fulfill the requirement of stretchability, but also produced the wrinkle structure on the PDMS. In this way, both the proper material and the microstructure can be accomplished with the single-step treating process. The output voltage, current, and surface charge density are increased by 100%, 810%, and 528% separately.

In addition to the contact material, the relative dielectric constant of the whole material can also influence the performance of the TENG [101] based on the capacitor model proposed by Niu et al. [102]. Hu et al. presented a TENG using a composite sponge PDMS as the dielectric, as shown in Fig. 5(d) [103]. This composite sponge PDMS is fabricated by first mixing different higher dielectric materials (SiO_2, TiO_2, $BaTiO_3$ and $SrTiO_3$) and NaCl with the pure PDMS and then dissolving the NaCl with water. The higher dielectric filler particles can increase the effective dielectric constant while the pores in the material can reduce the effective thickness of PDMS. Both of them is beneficial for increasing the capacitance, thus enhancing the output of TENG.
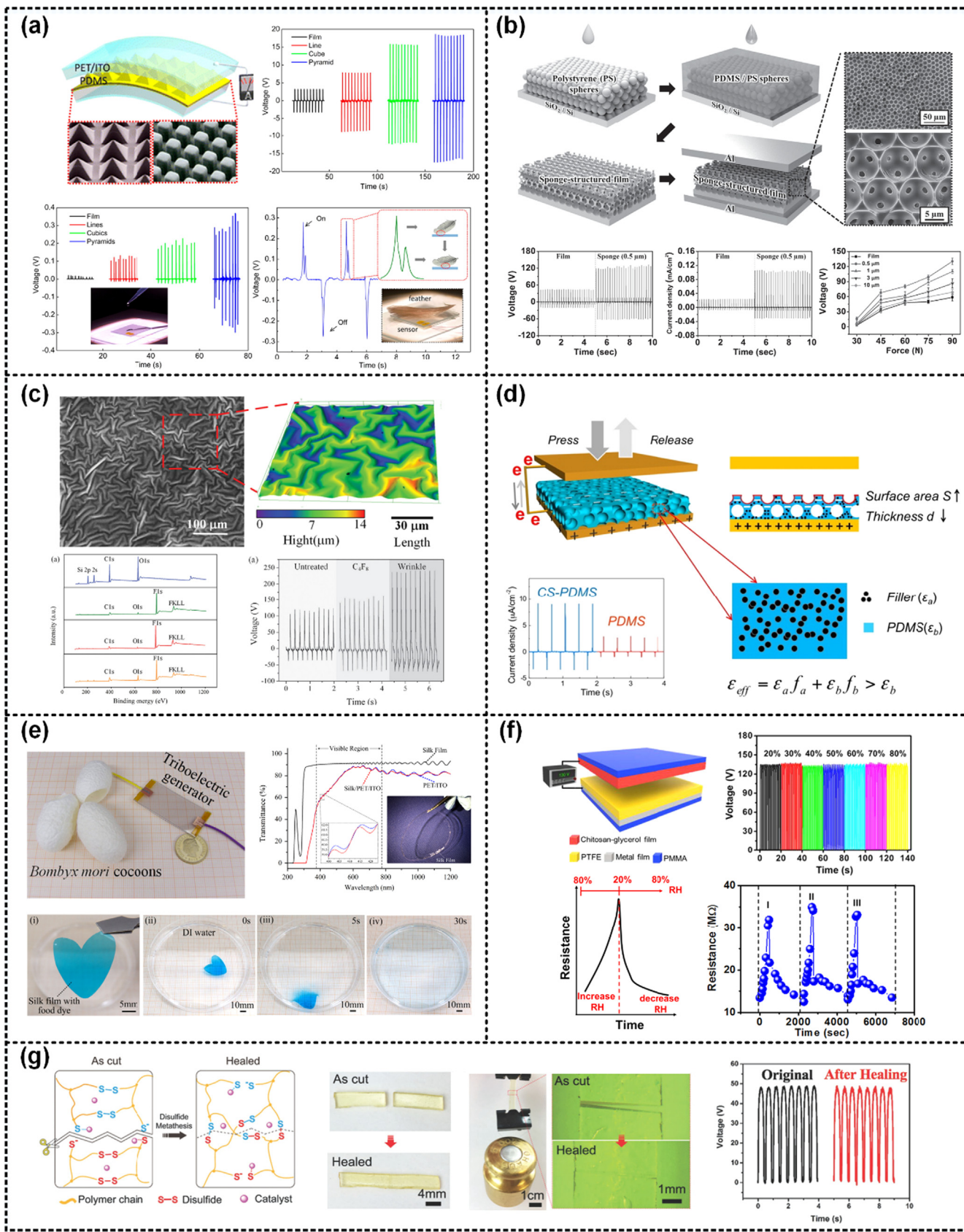
3.2.2. Other properties
Besides the sensing performance mentioned above, e-skin is expected to have more desired functions, which can better mimic the human skin. We will discuss several additional properties researchers pursued for incorporating into the e-skin in the following section.

3.2.2.1. Biocompatibility and biodegradability.
As e-skin requires intimate association with bio materials, biocompatibility is an important issue for design such device. Different from the man-made materials, nature materials can meet this requirement easily. Zhang et al. adopted the silk fibroin as the dielectric of TENG, which has a strong ability to lose electrons as shown in Fig. 5(e) [104]. Silk film can be controllably dissolved in aqueous solution, making it high environmental friendly. Compared with conventional materials like PET, PI, Teflon and PDMS, the output of silk based TENG is the largest, showing its potential for fabricating the high-performance devices. What's more, the silk fibroin owns high transparency to visible light, which can broaden its application fields like the transparent touch screen or invisible device.

3.2.2.2. Humidity-resistance.
Human skin can sense the mechanical signal even in humid environment. However, as mentioned above, TENG based self-powered sensor is sensitive to the humidity, which causes the sensor can't reflect the correct change accurately in humid environment [105]. To solve this problem, a chitosan-glycerol film was proposed by Lin et al. to work as the dielectric of TENG to avoid the variation caused by humidity, as shown in Fig. 5(f) [106]. With this material, the output characteristics of TENG remain stable when the relative humidity changes from 20% to 80%, which is very important for the device to work stably in the volatile environment.

3.2.2.3. Self-healing.
Natural skin has the outstanding ability to repair itself after incurring mechanical damage, which is difficult to realize in traditional electronics. The polymer based e-skin make the self-healing become possible by adopting new material in the design of e-skin [107]. Wang et al. proposed a self-healable, flexible and stretchable self-powered sensing device, which was fabricated by embedding a silver nanowire network in a disulfide bond containing vitrimer elastomer (Fig. 5(g)) [108]. Due to the dynamic disulfide exchange reaction in the vitrimer elastomer, the device enables fast structural/functional recovery and affords efficient shape configurability. This elastomer illustrates satisfying self-healing ability, which can recover to its original state at 90 °C with heating time of 30 min. The electrical performance can also be recovered after repairing damage, even after suffering severe deformation.

Fig. 5. Design of functional dielectric. (a) Various surface micro patterns to enhance the output of the TENG due to the enlarged contact area. Reproduced with permission from American Chemical Society (2012) [47]. (b) 3D sponge structured dielectric for improving the performance of TENG. Reproduced with permission from Wiley (2014) [99]. (c) A single-step fluorocarbon plasma treatment-induced wrinkle structure for high-performance TENG. Reproduced with permission from Wiley (2016) [100]. (d) Enhancing performance of TENG by filling different high dielectric nanoparticles into sponge structured PDMS film. Reproduced with permission from American Chemical Society (2015) [103]. (e) A silk- fibroin-based TENG which can dissolve into water with only 30 seconds. Reproduced with permission from Elsevier (2016) [104]. (f) A textile-based TENG with humidity-resistant output characteristic. Reproduced with permission from Elsevier (2018) [106]. (g) A Vitrimer elastomer-based self-healing TENG which can recover to its original state within only 5 seconds at 70℃. Reproduced with permission from Wiley (2018) [108].

4. Self-powered smart skin

The function of the self-powered e-skin can be very colorful according to its special designed configurations and detection methods. In the following section, we will introduce various functions of e-skin achieved by the TENG based self-powered sensors and self-powered e-skin system.

4.1. Self-powered sensor

Sensing is the core function for e-skin and TENG provides a convenient method for achieving this goal in a simple way without external battery. By designing plenty of configuration, various functions including pressure [56,109], positioning [58,110], strain [111,112], sliding [60,69] and so on [113,114] can be realized using TENGs with good performance.

4.1.1. Pressure sensor

Pressure sensor is the most common and significant sensor in the intelligent robot and so many groups have fabricated a lot of self-powered pressure sensors with fantastic performances [109]. The external mechanical stimuli can be reflected by the output magnitude of TENG because the pressure usually can increase the contact area, which can enhance the output of TENG. Zhu et al. reported an ultra-sensitive pressure sensor with sensitivity of 44 mV/Pa (0.09% Pa^{-1}) and a maximum touch sensitivity of 1.1 V/Pa (2.3% Pa^{-1}) in the extremely low-pressure region (< 0.15 kPa), as shown in Fig. 6(a) [56]. The key point of such high sensitivity is the top layer. The top layer is a fluorinated ethylene propylene (FEP) film, which is applied as an electrification layer contacted with a foreign object to generate triboelectric charges. Furthermore, the surface is modified to create vertically aligned polymer nanowires, which have an average diameter and length of 150 nm and 1.5 μm, respectively. This vertical aligned nanostructure plays a vital role in achieving high sensitivity for low pressure detection.

In general, TENG based pressure sensor is mainly designed to detect the dynamic signal because the output is a transient current flowing between two electrodes, which may lose some static information. To solve this problem, a flexible triboelectric active sensor was fabricated by Wang et al. [115], which can detect both static and dynamic pressure with different measurement approaches, as shown in Fig. 6(b). To be specific, the open-circuit voltage as well as the amount of transferred charge density was employed for the static detection, while the short-circuit current peak was adopted for the dynamic detection. Based on these sensing principles, this device demonstrates very good performance. The sensitivity can be as high as 0.31 kPa^{-1}, and the response time is less than 5 ms with a low pressure range as small as 2.1 Pa.

4.1.2. Position sensor

Positioning function is necessary to determine the exact location of the contact object. Sensor matrix is the most direct method to locate the position of the outer object [54,55]. Wang and his co-workers developed a self-powered sensor to track the trajectory, velocity, and acceleration of a moving object as shown in Fig. 6(c) [116]. This device is composed of a PTFE layer and Al film, working as the electrode for SE-TENG. The Al electrodes are matrix-distributed to locate the position of

a moving charged object. When the object moves close to an electrode, electrons will transfer between this electrode and ground, which can generate an electrical signal. If the interval between the neighboring electrodes is a constant, the displacement, velocity and acceleration of the object can all be measured by the basic kinematics.
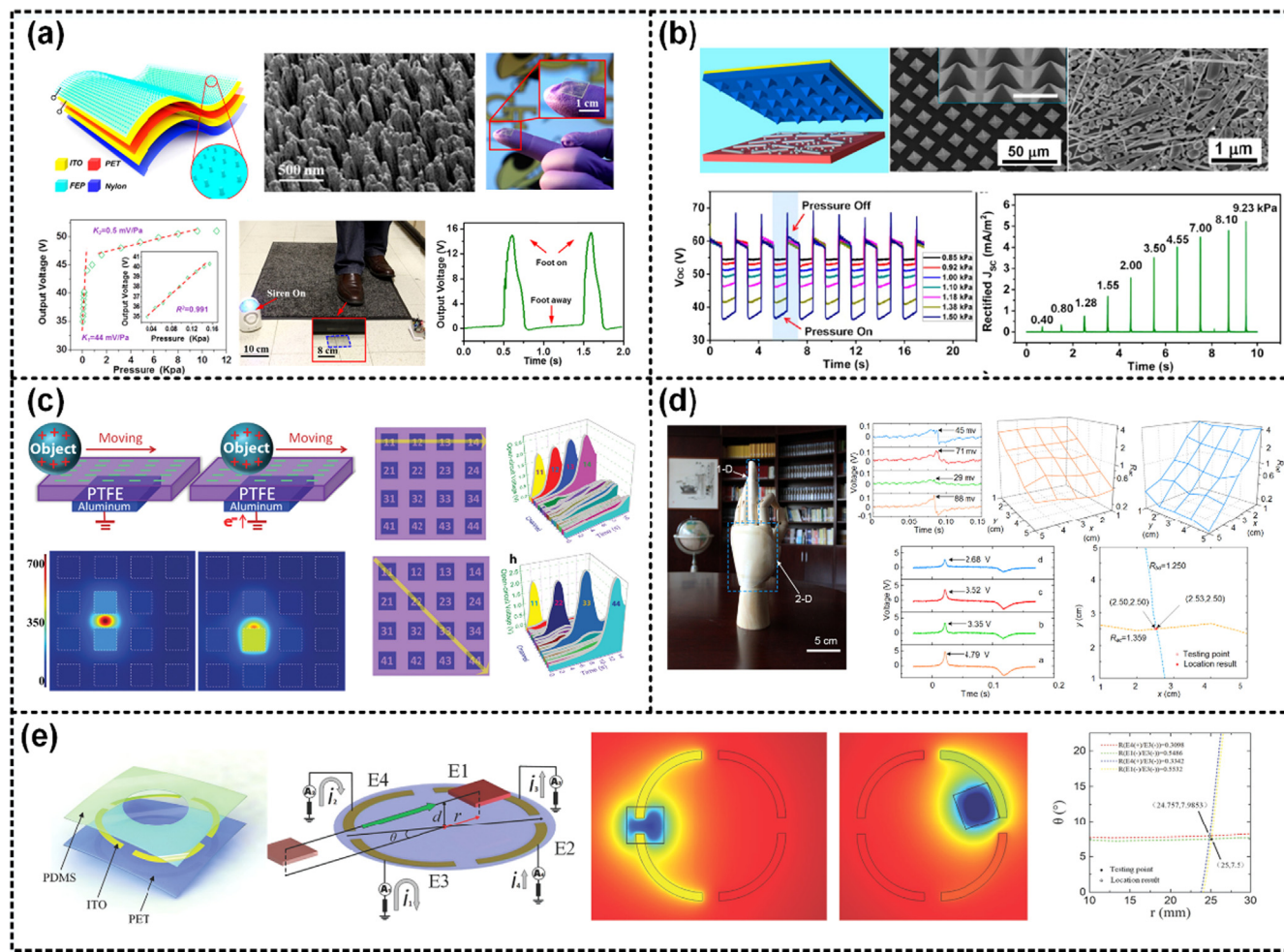
Although the addressing method can locate the exact position of the touch object, the number of electrodes would bring a lot of trouble in measurement when the number of pixels increases. Zhang el al proposed a self-powered analogue e-skin to solve this problem (Fig. 6(d) [58]. This analogue e-skin works based on the voltage ratios of opposite electrodes, which notably decreases the terminal number of the address nodes. For the 2D location, this device only need four electrodes to detect the whole plane. According the electrostatic induction, the output of the SF-TENG is associated with the distance from the contact point to the electrode. Due to this mechanism, the voltage ratio of two opposite electrodes can reflect the relative position along this direction. The resolution is as high as 1.2 mm at the plain surface.

Furthermore, the research group developed a noncontact location e-skin based on the similar mechanism. Four quarter annulus shaped ITO electrodes works as four SE-TENG, which can response to the movement of a charged object, as shown in Fig. 6(e) [110]. Based on the system of polar coordinates, the exact location of the noncontact object can be detected by the peak of voltages of the four SE-TENG. The resolution can reach 1.5 mm with a distance deviation of 0.4 mm. Spatial electrostatic induction allows users to have versatile inputs compared with traditional contact localizing methods.

4.1.3. Strain Sensor

Strain sensor is a kind of typical sensor, which is distinctive for the stretchable electronics [117]. It is necessary to consider the strain in the e-skin, however, for the traditional electronics, strain is not so significant as it is not obvious in the rigid materials. An active fiber based strain sensor was proposed by Zhou et al. (Fig. 7(a)) [112]. This sensor is composed of two kinds of pretreated cotton threads, one is CNT-coated cotton thread, and the other is PTFE and CNT-coated cotton thread. By entangling these two threads together to form a double-helixes and then coiled around a silicone, the whole device can detect the strain by calculating the amount of transferred charges between the two threads. The transferred charges vary linearly with the changed stimulated strains, and can avoid the influenced by the stimulated frequencies. This sensor can detect up to 25% strain, thus demonstrating the finger motion states.

Another digitalized strain sensor was proposed by Zhang et al., which can minimize the environment influence through the periodic signal of the TENG based sensor, as shown in Fig. 7(b) [111]. This device consists of a stretchable layer with two protrusions as an active part and a flexible layer with grated electrode as a static part. When the active part is stretched, the protrusion is moving to slide with the grated electrode, leading the output voltage changed periodically. Different from the above strain sensor based on the amount of transferred charges, the digitalized strain sensor will not influenced by the outer environment. The strain can be measured by just counting the number of peaks or valleys directly. Obviously, the resolution is determined by the configuration of the grated electrode.

Fig. 6. Self-powered pressure sensor and position sensor. (a) A self-powered, ultrasensitive, flexible pressure sensor with vertically aligned polymer nanowires. Reproduced with permission from American Chemical Society (2014) [56]. (b) A triboelectric based active sensor for self-powered static and dynamic pressure detection based on the open-circuit voltage and short-circuit current, respectively. Reproduced with permission from American Chemical Society (2013) [115]. (c) A self-powered sensor for tracking of object movement on a plane in a digital way. Reproduced with permission from Wiley (2014) [116]. (d) A self-powered analogue smart skin for positioning based on the amplitude ration of opposite electrodes. Reproduced with permission from American Chemical Society (2016) [58]. (e) A noncontact self-powered e-skin for motion detection with four quarter annulus electrodes which can calculate the displacement of the object with the voltage ratios under the system of polar coordinates. Reproduced with permission from Wiley (2018) [110].
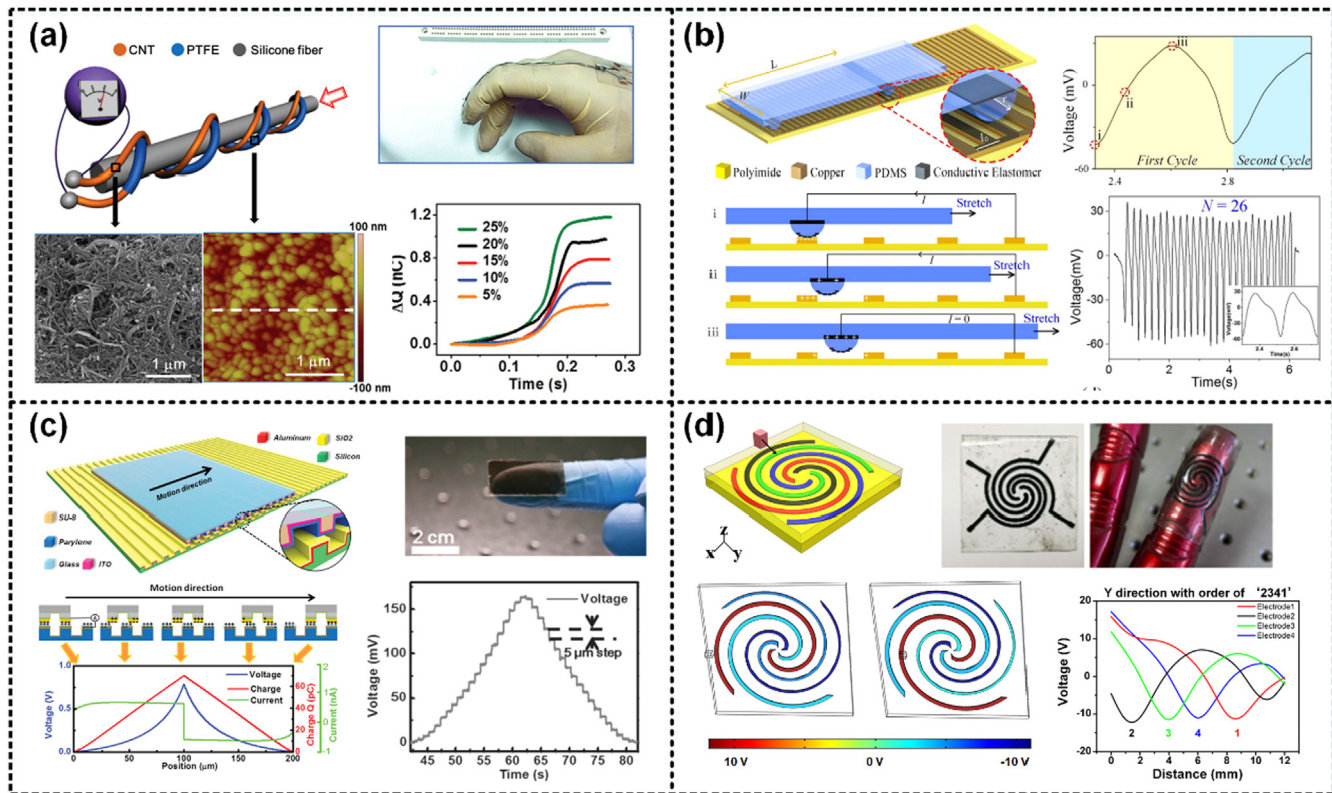
4.1.4. Sliding sensor

Sliding detection is also important for e-skin to detect horizontal movement of outer object. The first sliding displacement TENG based self-powered sensor was designed by Zhu et al. as shown in Fig. 7(c) [61]. This device is composed of two micro gratings with identical pattern. The grating at the bottom is made of an etched silicon wafer coated with Al and silicon dioxide. The top grating is the patterned SU-8 film on a glass slide coated with ITO and Parylene. The relative sliding motion between the two gratings leads to periodic separation, which generates the alternating output voltage. The one dimensional sliding displacement and speed can be detected using peak/zero-crossing counting method, which is robust against many environment effects. The resolution can be improved by reducing the size of the gratings.

Although the above sliding sensor can detect the displacement and the speed, it can only work in one dimension. In order to solve this problem, a fingerprint inspired spiral shaped pattern was developed by Chen et al. (Fig. 7(d)) [60]. The fingerprint inspired TENG consists of a PDMS substrate and four CNT-PDMS spiral electrodes, each of which works as an independent SE-TENG. Four electrodes are separately marked with a specific number. The pattern of electrodes is carefully designed to ensure no matter what direction an external object slides across the surface of the sensor, each SE-TENG can be activated one by

one. Due to the spiral shaped electrodes, the response sequence of the four SE-TENGs is dependent on the sliding direction, which provide a way for sliding direction detection. Similar to the above sliding displacement sensor, this fingerprint inspired sensor can also measure the distance and the speed by count the peak number of the output voltage, which provide a robust way for the sliding detection. By integrating the direction detection into the sliding sensing, this sensor can better describe the movement of the outer object.

In general, SE mode and FS mode are comparatively easier for designing the e-skin as their working mechanism don't need comparative separation, which can save a lot of space with simple and thin structure. The contact-separation (CS) mode and lateral sliding (LS) mode can also work as an e-skin if elaborately designed such as the work in Fig. 7(a). From the sensor aspect, digital type of TENG based e-skin, mainly including the positioning, strain and sliding, provides an easier way in real applications due to the simple measurement method. For the analog type of sensors, mainly including the pressure sensors, they can also work in real application with the proper method to protect them from the environmental interfere like the example in Fig. 5(g).

Fig. 7. Self-powered strain sensor and sliding sensor. (a) A stretchable self-powered fiber structured strain sensor based on the quantity of the transfer changes. Reproduced with permission from Wiley (2015) [112]. (b) A digitalized self-powered strain gauge for static and dynamic measurement. Reproduced with permission from Elsevier (2017) [111]. (c) A high resolution self-powered 1D sliding sensor based on micro-grated TENG. Reproduced with permission from Wiley (2013) [61]. (d) A multidirectional sliding detection self-powered sensor based on the fingerprint inspired structure. Reproduced with permission from Elsevier (2018) [60].

4.2. Self-powered e-skin system

Besides the self-powered sensor, self-powered skin system, consisting of energy harvester, energy storage and functional sensor, is also proposed to solve the energy problem in the e-skin application field if all the electronic devices can be attached on the surface of human skin or the robot while maintaining their functions under strain. According to the data from Samsung [118], the smart tablets and smart phones are the kinds of high power portable electronic devices and the power consumption is in the range of 50 mW^{-1} W. The power consumption of lower power electronic devices, mainly including the heartbeat sensor, pressure sensor, motion sensor and acceleration sensor, is in the range of 10–100 μW [119]. The power density of wearable TENG is in the range of 0.1–100 mW/m^2 with efficiency of 10–85% [120], which is very hopeful to supply energy for the traditional sensors and attracts lots of research groups to devote efforts in this self-powered system area [28]. The corresponding data is demonstrated in Figure S1 in Supporting information.

The whole system can be divided into two subsystems, the energy harvesting system and the energy supply system. The energy harvesting system consists of the energy harvester device and energy storage device [121–123] while the energy supply system consists of the energy storage device and functional sensor [124–127]. By integrating the two subsystems together, we can obtain a self-powered system to solve the energy problem in wearable electronics.

4.2.1. Energy harvesting system

Constructing a high-efficiency energy harvesting system is a significant issue and the main problem is how to integrate these two modulus together to make them working as a whole part. Song et al. reported a hybrid sandwich-shaped, self-charging power unit involving both the TENG and supercapacitor (SC). This energy harvesting system
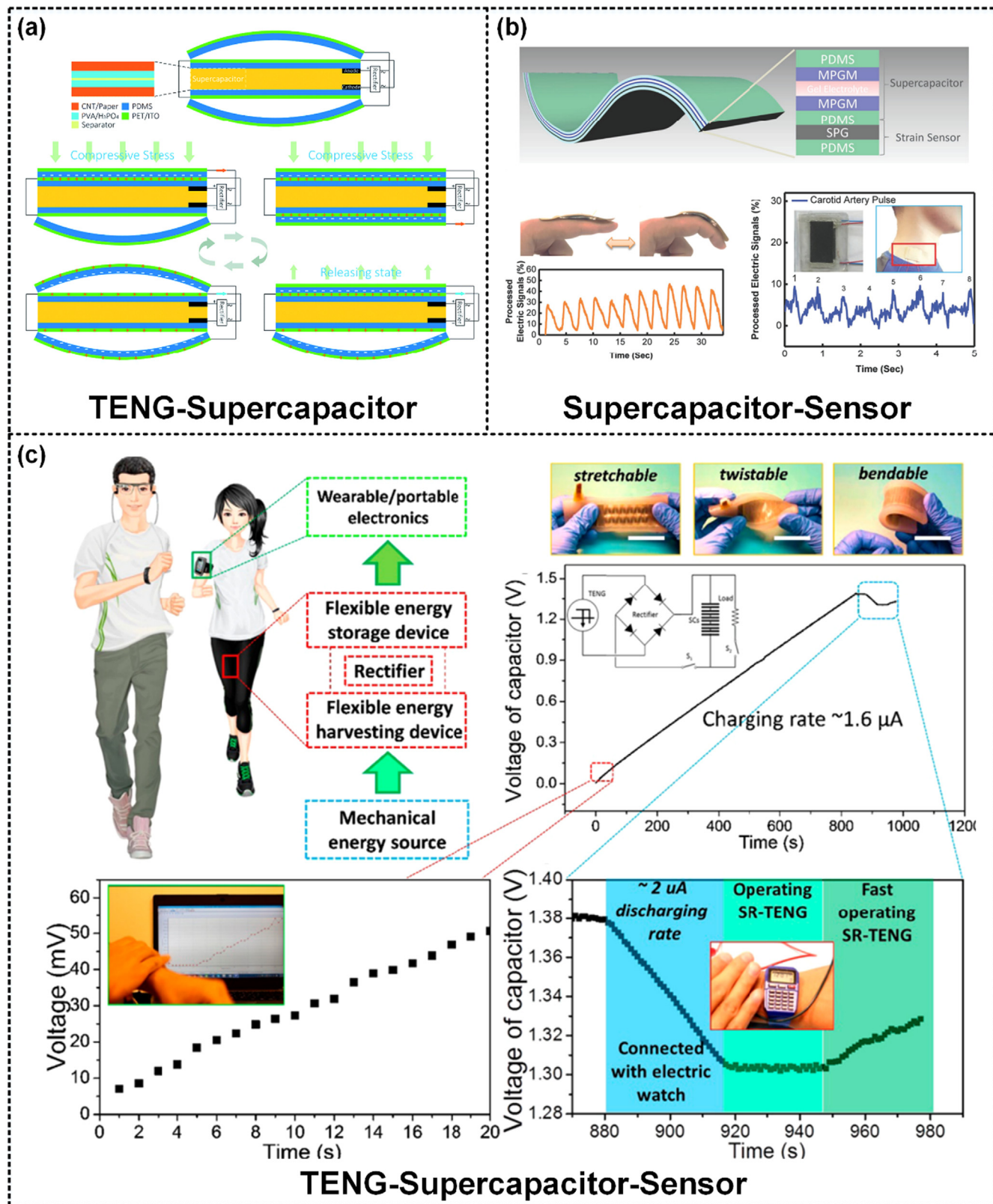
is shown in Fig. 8(a) [128]. The high degree of integration is realized through the TENG-SC-TENG design, which could take advantages of both the top and bottom surfaces of SC and greatly decrease the unit's volume. When compressive stress is applied on the surface of TENG, the mechanical energy can be converted into electrical energy and directly stored in the SC.

4.2.2. Energy supply system

Energy supply system mainly focus on the integration of energy storage device and functional sensor. Similarly, researchers hope that these two devices can be fabricated together to avoid the wiring problem in it. Fan and his co-workers proposed an energy supply system consisting of an ultralight and binder-free solid state supercapacitors and a wearable strain sensors as shown in Fig. 8(b) [129]. As the capacitor variance of the supercapacitor is sight under mechanical deformation, it can be stacked with the strain sensor together to conform on human skins and monitor some minor motion without other energy supply.

4.2.3. All-in-one system

The ultimate form of self-powered e-skin system is the integration of the three parts, energy harvester, energy storage device and wearable device, all of which can work smoothly even under stress. In 2016, Wang et al. proposed a prototype of an all-in-one self-powered system, which can be used for harvesting body motion energy under complex mechanical deformations, storing the mechanical energy and powering wearable electronics (Fig. 8(c)) [130]. With the kirigami structure, an ultra-stretchable paper based supercapacitor is fabricated to integrated with a shape-adaptive TENG consisting silicon rubber and AgNW electrodes. By assembling the SC into the TENG with a full-wave rectifier, this SC-TENG module can harvest hand flapping energy and continually powering a commercial electronic watch.

Fig. 8. Self-powered system. (a) Energy harvesting system consisting TENG and supercapacitor, which can generate energy from external stimuli and store the energy into the supercapacitor directly. Reproduced with permission from Royal Society of Chemistry (2016) [128] (b) Energy supply system consisting supercapacitor and sensor, which can drive the wearable electronic device with the wearable energy storage device without external battery Reproduced with permission from Wiley (2017) [129]. (c) All-in-one system which integrate the energy harvesting device, energy storage device and functional device together to form a self-powered system. Reproduced with permission from American Chemical Society (2016) [130].
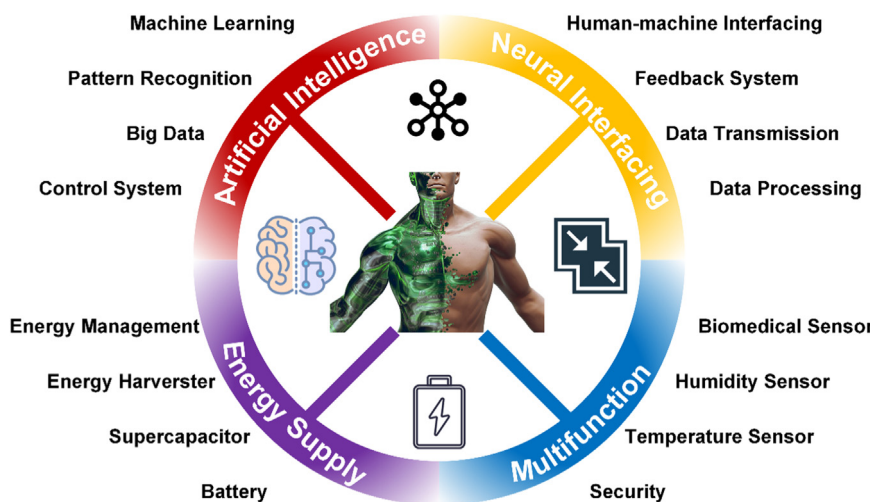
Fig. 9. Prospective of self-powered e-skin.

5. Conclusion and outlook

In the past decades, the development of new material and fabrication process make the electronics engineering bloom again from the traditional silicon based electronics to the polymer based stretchable electronics. This review focuses on the TENG based self-powered e-skin devices, which is beneficial for solving the energy supply problem of sensor networks in the stretchable electronic system. We firstly summarize the choice of the working modes, sensor types and detection modes, which are the fundamental point for designing a proper e-skin with the expected function. Furthermore, the method to mimic the properties of human skin, which must meets the demands of mechanical stretchability and electrical conductance at the same time, is reviewed from the electrode aspect and dielectric aspect, respectively. The material development and structure construction are two main approaches for making the conductor into stretchability. For the dielectric, the methods to improve the performance and endow more human skin functions like biocompatibility, self-healing and humidity-resistance are also stated. Furthermore, the state-of-the-art functional self-powered e-skins such as pressure sensor, position sensor, strain sensor and sliding sensor, and self-powered e-skin systems are demonstrated to discuss their great potential in different application fields.

A lot of progresses have been made in the self-powered sensor field, however, there are still some challenges hoped to be solved with the continuous efforts to make them more applicable (Fig. 9) [131–134]. Researchers have already begun to overcome these obstacles from different related fields like the multi-functional sensor system [135], energy management [136]. In the long term, the development of e-skin needs efforts from inter disciplinary research fields like neural interfacing, artificial intelligence and so on [137,138]. It is believed that the self-powered e-skin will develop more and more rapidly and play a vital role in the future electronic system, making e-skin technology applicable in both industry and people lives.

Acknowledgment

Appendix A. Supporting information

Supplementary data associated with this article can be found in the online version at doi:10.1016/j.nanoen.2018.11.061.

References

[1] M.L. Hammock, A. Chortos, B.C. Tee, J.B. Tok, Z. Bao, Adv. Mater. 25 (2013) 5997–6038.
[2] N. Gershenfeld, R. Krikorian, D. Cohen, Sci. Am. 291 (2004) 76–81.
[3] M.M. Shulaker, G. Hills, R.S. Park, R.T. Howe, K. Saraswat, H.S.P. Wong, S. Mitra, Nature 547 (2017) 74.
[4] X. Wang, L. Dong, H. Zhang, R. Yu, C. Pan, Z.L. Wang, Adv. Sci. 2 (2015) 1500169.
[5] A. Chortos, J. Liu, Z. Bao, Nat. Mater. 15 (2016) 937.
[6] Z. Ma, Science 333 (2011) 830–831.
[7] Q. Hua, J. Sun, H. Liu, R. Bao, R. Yu, J. Zhai, C. Pan, Z.L. Wang, Nat. Commun. 9 (2018) 244.
[8] D. Kang, P.V. Pikhitsa, Y.W. Choi, C. Lee, S.S. Shin, L. Piao, B. Park, K.-Y. Suh, T.-i. Kim, M. Choi, Nature 516 (2014) 222–226.
[9] C. Pang, J.H. Koo, A. Nguyen, J.M. Caves, M.G. Kim, A. Chortos, K. Kim, P.J. Wang, J.B.H. Tok, Z. Bao, Adv. Mater. 27 (2015) 634–640.
[10] W. Gao, S. Emaminejad, H.Y.Y. Nyein, S. Challa, K. Chen, A. Peck, H.M. Fahad, H. Ota, H. Shiraki, D. Kiriya, Nature 529 (2016) 509.
[11] T. Someya, Z.N. Bao, G.G. Malliaras, Nature 540 (2016) 379–385.
[12] J. Kim, M. Lee, H.J. Shim, R. Ghaffari, H.R. Cho, D. Son, Y.H. Jung, M. Soh, C. Choi, S. Jung, Nat. Commun. 5 (2014) 5747.
[13] M. Kaltenbrunner, T. Sekitani, J. Reeder, T. Yokota, K. Kuribara, T. Tokuhara, M. Drack, R. Schwödiauer, I. Graz, S. Bauer-Gogonea, S. Bauer, T. Someya, Nature 499 (2013) 458.
[14] H. Chen, Z. Su, Y. Song, X. Cheng, X. Chen, B. Meng, Z. Song, D. Chen, H. Zhang, Adv. Funct. Mater. 27 (2017) 1604434.
[15] D. Rus, M.T. Tolley, Nature 521 (2015) 467.
[16] M. Moravčík, M. Schmid, N. Burch, V. Lisý, D. Morrill, N. Bard, T. Davis, K. Waugh, M. Johanson, M. Bowling, Science 356 (2017) 508–513.
[17] Z.L. Wang, J. Chen, L. Lin, Energ. Environ. Sci. 8 (2015) 2250–2282.
[18] F.R. Fan, W. Tang, Z.L. Wang, Adv. Mater. 28 (2016) 4283–4305.
[19] Z.L. Wang, Sci. Am. 298 (2008) 82–87.
[20] Z.L. Wang, Adv. Mater. 24 (2012) 280–285.
[21] S. Wang, L. Lin, Z.L. Wang, Nano Energy 11 (2015) 436–462.
[22] Z.L. Wang, W. Wu, Angew. Chem. Int. Ed. 51 (2012) 11700–11721.
[23] F. Di Giacomo, A. Fakharuddin, R. Jose, T.M. Brown, Energ. Environ. Sci. 9 (2016) 3007–3035.
[24] L. Yang, Z.-G. Chen, M.S. Dargusch, J. Zou, Adv. Energy Mater. 8 (2018) 1701797.
[25] C.R. Valenta, G.D. Durgin, IEEE Microw. Mag. 15 (2014) 108–120.
[26] Z.L. Wang, J. Song, Science 312 (2006) 242–246.
[27] F.-R. Fan, Z.-Q. Tian, Z.L. Wang, Nano Energy 1 (2012) 328–334.
[28] X.-S. Zhang, M. Han, B. Kim, J.-F. Bao, J. Brugger, H. Zhang, Nano Energy 47 (2018) 410–426.
[29] Z.L. Wang, ACS Nano 7 (2013) 9533–9557.
[30] F.R. Fan, W. Tang, Y. Yao, J.J. Luo, C. Zhang, Z.L. Wang, Nanotechnology 25 (2014).
[31] C. Zhang, W. Tang, C. Han, F. Fan, Z.L. Wang, Adv. Mater. 26 (2014) 3580–3591.
[32] C. Dagdeviren, Z. Li, Z.L. Wang, Annu. Rev. Biomed. Eng. 19 (2017) 85–108.
[33] G. Zhu, B. Peng, J. Chen, Q. Jing, Z. Lin Wang, Nano Energy 14 (2015) 126–138.
[34] R. Hinchet, W. Seung, S.-W. Kim, ChemSusChem 8 (2015) 2327–2344.
[35] J.W. Lee, B.U. Ye, J.M. Baik, Apl. Mater. 5 (2017) 073802.
[36] N. Zhang, C. Tao, X. Fan, J. Chen, J. Mater. Res. 32 (2017) 1628–1646.
[37] X.-S. Zhang, M.-D. Han, B. Meng, H.-X. Zhang, Nano Energy 11 (2015) 304–322.
[38] X.-S. Zhang, M. Su, J. Brugger, B. Kim, Nano Energy 33 (2017) 393–401.
[39] X.-S. Zhang, M.-D. Han, R.-X. Wang, F.-Y. Zhu, Z.-H. Li, W. Wang, H.-X. Zhang, Nano Lett. 13 (2013) 1168–1172.
[40] S. Wang, L. Lin, Z.L. Wang, Nano Lett. 12 (2012) 6339–6346.
[41] G. Zhu, J. Chen, Y. Liu, P. Bai, Y.S. Zhou, Q. Jing, C. Pan, Z.L. Wang, Nano Lett. 13

(2013) 2282–2289.

[42] S. Wang, L. Lin, Y. Xie, Q. Jing, S. Niu, Z.L. Wang, Nano Lett. 13 (2013) 2226–2233.

[43] Y. Yang, H. Zhang, J. Chen, Q. Jing, Y.S. Zhou, X. Wen, Z.L. Wang, ACS Nano 7 (2013) 7342–7351.

[44] B. Meng, W. Tang, Z.-h. Too, X. Zhang, M. Han, W. Liu, H. Zhang, Energ. Environ. Sci. 6 (2013) 3235–3240.

[45] S. Wang, Y. Xie, S. Niu, L. Lin, Z.L. Wang, Adv. Mater. 26 (2014) 2818–2824.

[46] G. Zhu, C. Pan, W. Guo, C.-Y. Chen, Y. Zhou, R. Yu, Z.L. Wang, Nano Lett. 12 (2012) 4960–4965.

[47] F.-R. Fan, L. Lin, G. Zhu, W. Wu, R. Zhang, Z.L. Wang, Nano Lett. 12 (2012) 3109–3114.

[48] S.M. Niu, Y. Liu, S.H. Wang, L. Lin, Y.S. Zhou, Y.F. Hu, Z.L. Wang, Adv. Funct. Mater. 24 (2014) 3332–3340.

[49] B. Meng, X.L. Cheng, X.S. Zhang, M.D. Han, W. Liu, H.X. Zhang, Appl. Phys. Lett. 104 (2014).

[50] S.M. Niu, S.H. Wang, Y. Liu, Y.S. Zhou, L. Lin, Y.F. Hu, K.C. Pradel, Z.L. Wang, Energ. Environ. Sci. 7 (2014) 2339–2349.

[51] Y.N. Xie, S.H. Wang, S.M. Niu, L. Lin, Q.S. Jing, J. Yang, Z.Y. Wu, Z.L. Wang, Adv. Mater. 26 (2014) 6599–6607.

[52] G.H. Lim, S.S. Kwak, N. Kwon, T. Kim, H. Kim, S.M. Kim, S.W. Kim, B. Lim, Nano Energy 42 (2017) 300–306.

[53] Y.J. Su, G. Zhu, W.Q. Yang, J. Yang, J. Chen, Q.S. Jing, Z.M. Wu, Y.D. Jiang, Z.L. Wang, ACS Nano 8 (2014) 3843–3850.

[54] Y. Yang, H.L. Zhang, Z.H. Lin, Y.S. Zhou, Q.S. Jing, Y.J. Su, J. Yang, J. Chen, C.G. Hu, Z.L. Wang, ACS Nano 7 (2013) 9213–9222.

[55] X.D. Wang, H.L. Zhang, L. Dong, X. Han, W.M. Du, J.Y. Zhai, C.F. Pan, Z.L. Wang, Adv. Mater. 28 (2016) 2896–2903.

[56] G. Zhu, W.Q. Yang, T. Zhang, Q. Jing, J. Chen, Y.S. Zhou, P. Bai, Z.L. Wang, Nano Lett. 14 (2014) 3208–3213.

[57] Z. Ren, J. Nie, J. Shao, Q. Lai, L. Wang, J. Chen, X. Chen, Z.L. Wang, Adv. Funct. Mater. 28 (2018) 1802989.

[58] M. Shi, J. Zhang, H. Chen, M. Han, S.A. Shankaregowda, Z. Su, B. Meng, X. Cheng, H. Zhang, ACS Nano 10 (2016) 4083–4091.

[59] J. Zhang, Z. Song, H. Guo, Y. Song, B. Yu, H. Zhang, IEEE Trans. Nanotechnol. 17 (2018) 460–466.

[60] H. Chen, Y. Song, H. Guo, L. Miao, X. Chen, Z. Su, H. Zhang, Nano Energy 51 (2018) 496–503.

[61] Y.S. Zhou, G. Zhu, S. Niu, Y. Liu, P. Bai, Q. Jing, Z.L. Wang, Adv. Mater. 26 (2014) 1719–1724.

[62] S. Wang, S. Niu, J. Yang, L. Lin, Z.L. Wang, ACS Nano 8 (2014) 12004–12013.

[63] J. Yang, J. Chen, Y. Liu, W. Yang, Y. Su, Z.L. Wang, ACS Nano 8 (2014) 2649–2657.

[64] X. Chen, H. Guo, H. Wu, H. Chen, Y. Song, Z. Su, H. Zhang, Nano Energy 49 (2018) 51–58.

[65] L. Lin, S. Wang, S. Niu, C. Liu, Y. Xie, Z.L. Wang, ACS Appl. Mater. Interfaces 6 (2014) 3031–3038.

[66] L. Lin, S. Wang, Y. Xie, Q. Jing, S. Niu, Y. Hu, Z.L. Wang, Nano Lett. 13 (2013) 2916–2923.

[67] H. Zhang, Y. Yang, Y. Su, J. Chen, K. Adams, S. Lee, C. Hu, Z.L. Wang, Adv. Funct. Mater. 24 (2014) 1401–1407.

[68] Y. Yang, H.L. Zhang, R.Y. Liu, X.N. Wen, T.C. Hou, Z.L. Wang, Adv. Energy Mater. 3 (2013) 1563–1568.

[69] H.T. Chen, L.M. Miao, Z.M. Su, Y. Song, M.D. Han, X.X. Chen, X.L. Cheng, D.M. Chen, H.X. Zhang, Nano Energy 40 (2017) 65–72.

[70] S. Zhao, J. Li, D. Cao, G. Zhang, J. Li, K. Li, Y. Yang, W. Wang, Y. Jin, R. Sun, C.-P. Wong, ACS Appl. Mater. Interfaces 9 (2017) 12147–12164.

[71] D.-H. Kim, R. Ghaffari, N. Lu, J.A. Rogers, Annu. Rev. Biomed. Eng. 14 (2012) 113–128.

[72] X. Yu, B. Mahajan, W. Shou, H. Pan, Micromachines 8 (2017) 7.

[73] S. Iijima, Nature 354 (1991) 56.

[74] K.S. Novoselov, A.K. Geim, S.V. Morozov, D. Jiang, Y. Zhang, S.V. Dubonos, I.V. Grigorieva, A.A. Firsov, Science 306 (2004) 666–669.

[75] S. Park, H. Kim, M. Vosgueritchian, S. Cheon, H. Kim, J.H. Koo, T.R. Kim, S. Lee, G. Schwartz, H. Chang, Z.A. Bao, Adv. Mater. 26 (2014) 7324–7332.

[76] S. Kim, M.K. Gupta, K.Y. Lee, A. Sohn, T.Y. Kim, K.S. Shin, D. Kim, S.K. Kim, K.H. Lee, H.J. Shin, D.W. Kim, S.W. Kim, Adv. Mater. 26 (2014) 3918–3925.

[77] T. Araki, M. Nogi, K. Suganuma, M. Kogure, O. Kirihara, IEEE Electron Device Lett. 32 (2011) 1424–1426.

[78] J. Ge, H.-B. Yao, X. Wang, Y.-D. Ye, J.-L. Wang, Z.-Y. Wu, J.-W. Liu, F.-J. Fan, H.-L. Gao, C.-L. Zhang, S.-H. Yu, Angew. Chem. Int. Ed. 52 (2013) 1654–1659.

[79] Z. Yu, Q. Zhang, L. Li, Q. Chen, X. Niu, J. Liu, Q. Pei, Adv. Mater. 23 (2011) 664–668.

[80] Y.C. Lai, J. Deng, R. Liu, Y.C. Hsiao, S.L. Zhang, W. Peng, H.M. Wu, X. Wang, Z.L. Wang, Adv. Mater. 30 (2018).

[81] Y.-C. Lai, J. Deng, S. Niu, W. Peng, C. Wu, R. Liu, Z. Wen, Z.L. Wang, Adv. Mater. 28 (2016) 10024–10032.

[82] X.Y. Chen, Y.L. Wu, J.J. Shao, T. Jiang, A.F. Yu, L. Xu, Z.L. Wang, Small 13 (2017).

[83] S.M. Li, W.B. Peng, J. Wang, L. Lin, Y.L. Zi, G. Zhang, Z.L. Wang, ACS Nano 10 (2016) 7973–7981.

[84] S. Wagner, S.P. Lacour, J. Jones, P.H.I. Hsu, J.C. Sturm, T. Li, Z. Suo, Phys. E Low. Dimens. Syst. Nanostruct. 25 (2004) 326–334.

[85] C. Keplinger, J.Y. Sun, C.C. Foo, P. Rothemund, G.M. Whitesides, Z.G. Suo, Science 341 (2013) 984–987.

[86] J.Y. Sun, C. Keplinger, G.M. Whitesides, Z.G. Suo, Adv. Mater. 26 (2014) 7608–7614.

[87] X. Pu, M.M. Liu, X.Y. Chen, J.M. Sun, C.H. Du, Y. Zhang, J.Y. Zhai, W.G. Hu, Z.L. Wang, Sci. Adv. 3 (2017).

[88] J. Jones, S.P. Lacour, S. Wagner, Z.G. Suo, J. Vac. Sci. Technol. A 22 (2004) 1723–1725.

[89] L.M. Miao, X.L. Cheng, H.T. Chen, Y. Song, H. Guo, J.X. Zhang, X.X. Chen, H.X. Zhang, J. Micromech. Microeng. 28 (2018).

[90] D. Hong, J. Jeong, Y.M. Choi, J. Micromech. Microeng. 25 (2015).

[91] Y.C. Lai, J. Deng, S.L. Zhang, S. Niu, H. Guo, Z.L. Wang, Adv. Funct. Mater. 27 (2017).

[92] P.K. Yang, Z.H. Lin, K.C. Pradel, L. Lin, X.H. Li, X.N. Wen, J.H. He, Z.L. Wang, ACS Nano 9 (2015) 901–907.

[93] C.S. Wu, X. Wang, L. Lin, H.Y. Guo, Z.L. Wang, ACS Nano 10 (2016) 4652–4659.

[94] Z.Z. Zhao, C. Yan, Z.X. Liu, X.L. Fu, L.M. Peng, Y.F. Hu, Z.J. Zheng, Adv. Mater. 28 (2016) 10267–10274.

[95] W. Zeng, X.-M. Tao, S. Chen, S. Shang, H.L.W. Chan, S.H. Choy, Energy Environ. Sci. 6 (2013) 2631–2638.

[96] R. Cao, X.J. Pu, X.Y. Du, W. Yang, J.N. Wang, H.Y. Guo, S.Y. Zhao, Z.Q. Yuan, C. Zhang, C.J. Li, Z.L. Wang, ACS Nano 12 (2018) 5190–5196.

[97] K.Y. Lee, H.J. Yoon, T. Jiang, X.N. Wen, W. Seung, S.W. Kim, Z.L. Wang, Adv. Energy Mater. 6 (2016).

[98] P.K. Yang, L. Lin, F. Yi, X.H. Li, K.C. Pradel, Y.L. Zi, C.I. Wu, J.H. He, Y. Zhang, Z.L. Wang, Adv. Mater. 27 (2015) 3817–3824.

[99] K.Y. Lee, J. Chun, J.H. Lee, K.N. Kim, N.R. Kang, J.Y. Kim, M.H. Kim, K.S. Shin, M.K. Gupta, J.M. Baik, S.W. Kim, Adv. Mater. 26 (2014) 5037–5042.

[100] X.L. Cheng, B. Meng, X.X. Chen, M.D. Han, H.T. Chen, Z.M. Su, M.Y. Shi, H.X. Zhang, Small 12 (2016) 229–236.

[101] X.M. He, H.Y. Guo, X.L. Yue, J. Gao, Y. Xia, C.G. Hu, Nanoscale 7 (2015) 1896–1903.

[102] S. Niu, Z.L. Wang, Nano Energy 14 (2015) 161–192.

[103] J. Chen, H.Y. Guo, X.M. He, G.L. Liu, Y. Xi, H.F. Shi, C.G. Hu, ACS Appl. Mater. Interfaces 8 (2016) 736–744.

[104] X.S. Zhang, J. Brugger, B. Kim, Nano Energy 20 (2016) 37–47.

[105] X. Chen, L. Miao, H. Guo, H. Chen, Y. Song, Z. Su, H. Zhang, Appl. Phys. Lett. 112 (2018) 203902.

[106] Y.T. Jao, P.K. Yang, C.M. Chiu, Y.J. Lin, S.W. Chen, D. Choi, Z.H. Lin, Nano Energy 50 (2018) 513–520.

[107] J.M. Sun, X. Pu, M.M. Liu, A.F. Yu, C.H. Du, J.Y. Zhai, W.G. Hu, Z.L. Wang, ACS Nano 12 (2018) 6147–6155.

[108] J.N. Deng, X. Kuang, R.Y. Liu, W.B. Ding, A.C. Wang, Y.C. Lai, K. Dong, Z. Wen, Y.X. Wang, L.L. Wang, H.J. Qi, T. Zhang, Z.L. Wang, Adv. Mater. 30 (2018).

[109] S.W. Chen, X. Cao, N. Wang, L. Ma, H.R. Zhu, M. Willander, Y. Jie, Z.L. Wang, Adv. Energy Mater. 7 (2017).

[110] H.X. Wu, Z.M. Su, M.Y. Shi, L.M. Miao, Y. Song, H.T. Chen, M.D. Han, H.X. Zhang, Adv. Funct. Mater. 28 (2018).

[111] Z.M. Su, H.X. Wu, H.T. Chen, H. Guo, X.L. Cheng, Y. Song, X.X. Chen, H.X. Zhang, Nano Energy 42 (2017) 129–137.

[112] J.W. Zhong, Q.Z. Zhong, Q.Y. Hu, N. Wu, W.B. Li, B. Wang, B. Hu, J. Zhou, Adv. Funct. Mater. 25 (2015) 1798–1803.

[113] X. Chen, Y. Song, H. Chen, J. Zhang, H. Zhang, J. Mater. Chem. A 5 (2017) 12361–12368.

[114] M. Han, B. Yu, G. Qiu, H. Chen, Z. Su, M. Shi, B. Meng, X. Cheng, H. Zhang, J. Mater. Chem. A 3 (2015) 7382–7388.

[115] L. Lin, Y.N. Xie, S.H. Wang, W.Z. Wu, S.M. Niu, X.N. Wen, Z.L. Wang, ACS Nano 7 (2013) 8266–8274.

[116] F. Yi, L. Lin, S.M. Niu, J. Yang, W.Z. Wu, S.H. Wang, Q.L. Liao, Y. Zhang, Z.L. Wang, Adv. Funct. Mater. 24 (2014) 7488–7494.

[117] S.L. Zhang, Y.C. Lai, X. He, R.Y. Liu, Y.L. Zi, Z.L. Wang, Adv. Funct. Mater. 27 (2017).

[118] K.-E. Byun, M.-H. Lee, Y. Cho, S.-G. Nam, H.-J. Shin, S. Park, Apl. Mater. 5 (2017) 074107.

[119] M. Ha, J. Park, Y. Lee, H. Ko, ACS Nano 9 (2015) 3421–3427.

[120] Y. Zi, Z.L. Wang, Apl. Mater. 5 (2017) 074103.

[121] J. Kim, J.-H. Lee, J. Lee, Y. Yamauchi, C.H. Choi, J.H. Kim, Apl. Mater. 5 (2017) 073804.

[122] J.-H. Lee, J. Kim, T.Y. Kim, M.S. Al Hossain, S.-W. Kim, J.H. Kim, J. Mater. Chem. A 4 (2016) 7983–7999.

[123] X. Pu, W. Hu, Z.L. Wang, Small 14 (2018) 1702817.

[124] Y. Song, H. Chen, Z. Su, X. Chen, L. Miao, J. Zhang, X. Cheng, H. Zhang, Small 13 (2017) 1702091.

[125] X. Li, X. Li, J. Cheng, D. Yuan, W. Ni, Q. Guan, L. Gao, B. Wang, Nano Energy 21 (2016) 228–237.

[126] J. Yun, Y. Lim, G.N. Jang, D. Kim, S.-J. Lee, H. Park, S.Y. Hong, G. Lee, G. Zi, J.S. Ha, Nano Energy 19 (2016) 401–414.

[127] R. Guo, J. Chen, B. Yang, L. Liu, L. Su, B. Shen, X. Yan, Adv. Funct. Mater. 27 (2017) 1702394.

[128] Y. Song, X.L. Cheng, H.T. Chen, J.H. Huang, X.X. Chen, M.D. Han, Z.M. Su, B. Meng, Z.J. Song, H.X. Zhang, J. Mater. Chem. A 4 (2016) 14298–14306.

[129] W.G. Li, X.B. Xu, C. Liu, M.C. Tekell, J. Ning, J.H. Guo, J.C. Zhang, D.L. Fan, Adv. Funct. Mater. 27 (2017).

[130] H.Y. Guo, M.H. Yeh, Y.C. Lai, Y.L. Zi, C.S. Wu, Z. Wen, C.G. Hu, Z.L. Wang, ACS Nano 10 (2016) 10580–10588.

[131] G.-Z. Yang, J. Bellingham, P.E. Dupont, P. Fischer, L. Floridi, R. Full, N. Jacobstein, V. Kumar, M. McNutt, R. Merrifield, B.J. Nelson, B. Scassellati, M. Taddeo, R. Taylor, M. Veloso, Z.L. Wang, R. Wood, Sci. Robot. 3 (2018).

[132] S.M. Won, E. Song, J. Zhao, J. Li, J. Rivnay, J.A. Rogers, Adv. Mater. 30 (2018) 1800534.

[133] S.-K. Kang, J. Koo, Y.K. Lee, J.A. Rogers, Acc. Chem. Res. 51 (2018) 988–998.
[134] J. Heikenfeld, A. Jajack, J. Rogers, P. Gutruf, L. Tian, T. Pan, R. Li, M. Khine, J. Kim, J. Wang, J. Kim, Lab a Chip 18 (2018) 217–248.
[135] H. Chen, Z. Su, Y. Song, X. Cheng, X. Chen, B. Meng, Z. Song, D. Chen, H. Zhang, Adv. Funct. Mater. 27 (2017) (1604434-n/a).
[136] X.L. Cheng, L.M. Miao, Y. Song, Z.M. Su, H.T. Chen, X.X. Chen, J.X. Zhang, H.X. Zhang, Nano Energy 38 (2017) 448–456.
[137] A. Chortos, J. Liu, Z.A. Bao, Nat. Mater. 15 (2016) 937–950.
[138] Y. Song, J. Zhang, H. Guo, X. Chen, Z. Su, H. Chen, X. Cheng, H. Zhang, Appl. Phys. Lett. 111 (2017) 073901.

Xiao-Liang Cheng received the B.S. degree from the University of Electronic Science and Technology of China, Chengdu, in 2014. He is currently pursuing the Ph.D. degree at the National Key Laboratory of Nano/Micro Fabrication Technology, Peking University, Beijing, China. His research interests mainly include design and fabrication of nanogenerator and mechanical energy harvester.

Haotian Chen received the B.S. degree in Dalian University of Technology, China, and Ph.D. degree in Peking University. Currently he is a postdoctoral researcher at Texas A&M University, USA. His research work is focused on energy harvesting, stretchable electronic sensors and biosensors.

Haixia Zhang is currently a Professor with the Institute of Microelectronics, Peking University, Beijing, China. She received the Ph.D. degree in mechanical engineering from Huazhong University of Science and Technology, Wuhan, China, in 1998. She joined Peking University in 2001 after her post-doctoral research in Tsinghua University. Her research interests include MEMS and energy harvesting technology. She has served on the General Chair of the IEEE NEMS 2013 Conference, the Organizing Chair of Transducers'11. She is the Founder and General Chair of the International Contest of Innovation (iCAN) which was launched in 2007.

Yu Song received the B.S. degree in Electronic Science & Technology from Huazhong University of Science and Technology, China, in 2015. He is currently pursuing thePh.D. degree at the National Key Laboratory of Nano/Micro Fabrication Technology, Peking University, Beijing, China. He majors in MEMS and his research is focusing on wearable sensors and self-charging power system.